Discovery of a Unique Extracellular Polysaccharide in Members of the Pathogenic *Bacillus* that can Co-form with Spores

Zi Li[1,2], Soyoun Hwang[1], and Maor Bar-Peled[1,2,$]

From the Complex Carbohydrate Research Center[1] and Departments of Plant Biology[2], University of Georgia, Athens, Georgia 30602

Running title: *pzX an EPS surfactant and adherence of Bacillus*

[$]To whom correspondence should be addressed: Complex Carbohydrate Research Center, 315 Riverbend Rd., Athens, GA 30602. Tel.: 706-542-2062; Fax: 706-542-4412; E-mail: peled@ccrc.uga.edu.

Key words: Bacillus, sporulation, polysaccharides, glycobiology, biofilm, biosurfactant, exopolysaccharides (EPS), pzX, XylNAc, GlcNAcA

ABSTRACT

An exopolysaccharide, produced during late stage of stationary growth phase, was discovered and purified from the culture medium of *Bacillus cerues*, *B. anthracis*, and *B. thuringiensis* when strains were grown in a defined nutrient medium that induces biofilm. Two-dimensional NMR structural characterization of the polysaccharide, named pzX, revealed that it is composed of an unusual three amino-sugar sequence repeat of [-*3)*XylNAc4OAc(*α1-3)*GlcNAcA4OAc(*α1-3)*XylNAc(*α1*-]$_n$. The sugar residue XylNAc had never been previously described in any glycan structure. The XNAC operon that contains the genes for the assembly of pzX is also unique and so far identified only in members of the *Bacillus cereus* sensu lato group. Microscopic and biochemical analyses indicate that pzX co-forms during sporulation, such that upon the release of the spore to the extracellular milieu it becomes surrounded by pzX. The relative amounts of pzX produced can be manipulated by specific nutrient in the medium, but rich medium appears to suppress pzX formation. pzX has unique characteristics: a surfactant property that lowers surface tension, a cell/spore antiaggregant, and an adherence property that increases spores binding to surfaces. pzX in *Bacillus* could represent a trait shared by many spore-producing microorganisms. It suggests pzX is an active player in spore physiology and may provide new insights to the successful survival of the *B. cereus* species in natural environments or in the hosts.

INTRODUCTION

In 1881 Louis Pasteur developed the first vaccine for anthrax, the devastating disease caused by *Bacillus anthracis*, a Gram-positive endospore forming bacterium. Since then, outbreaks of anthrax affecting humans and animals have dramatically decreased (1,2); although infrequent incidents have been reported (3). However, letters containing *B. anthracis* spores sent by mail to US officials a week after the September 11, 2001 attack, led to public fear of infection and the use of its spores as a bioweapon agent (4). *B. anthracis*, although elicits different disease phenotypes, is closely related in terms of gene content and synteny (5) to other *Bacillus* species collectively named *Bacillus cereus sensu lato* (6) or *Bacillus cereus* group. These highly related *Bacilli* are able to colonize in diverse hosts including insects and mammals, and they are commonly found in soil, water, and depending on the specie in cadavers, vegetation and food. In addition to *B. anthracis*, this group includes *B. cereus*, recognized as a cause of food poisoning toxins, and *B. thuringiensis* that produces insecticidal proteins. In the past 15 years, several *B. cereus* strains were reported to cause severe anthrax-like disease in humans (7,8) and apes (9). Some of these virulent strains while retaining *B. cereus* diagnostic phenotypes harbor plasmids similar to the toxin and capsule virulence plasmids pXO1 and pXO2 present in *B. anthracis* (10-12). Hence, it is no wonder that the need to distinguish these *Bacillus* strains has led to a massive genome sequencing effort around the globe. In addition to 57 *Bacillus*

genome sequenced deposited in Genbank until 2009 (13), 94 environmental *Bacillus* genome sequences from the U.S. were added in 2013 (6); followed in 2014 by 122 sequences of French *Bacillus* strains (14) and more recently, in 2015, a Danish genome effort provide sequences of 41 isolates of *Bacillus* (15). These 314 *Bacillus* genome sequences should provide information to discriminate the different sub-groups of *Bacillus*.

Common to members of the *B. cereus* group is the formation of spores that are resilient to heat and chemicals and have the ability to survive for long duration (16). Another trait that raises serious concerns for health organizations is the ability of *Bacillus* to develop and live within a biofilm. Bacterial biofilms, in general, require special attention for the food industry, as they can be a source of persistent contamination leading to food spoilage and to the transmission of diseases (17). Indeed, *Bacillus cereus* spores and, to a lesser extent, vegetative cells embedded in biofilm are more protected against sanitizers (18,19). In bacterial species that were studied, biofilm provides means for the bacterial cell to attach and adhere to a variety of surfaces (both natural and man-made)(20,21). In *Staphylococcus* and *Pseudomonas*, it was suggested that cells imbedded in biofilm promote the survival of bacteria by forming a niche where bacteria can evade recognition by the host immune system (22,23); however, less is known regarding the myriad roles of biofilm in *Bacillus cereus* group. Biofilms form an extracellular polymeric matrix that is comprised of exopolysaccharides (EPS), proteins, lipids, and nucleic acids (24,25). A rigid biofilm structure from the motile model bacterium, *B. subtilis,* has extremely liquid and gas repellent properties; and mutation in biofilms formation suggested the involvement of EPS (26). While extended genetic research led to identification of numerous biosynthetic and regulatory genes involved in EPS formation in *B. subtilis* biofilm, less is known about biofilm formation in members of the pathogenic *B. cereus* group. Hence, despite differences in their pathogenicity, the exact nature of biofilm produced by this group of *Bacillus* and the repertoire of polysaccharide molecules made remain largely unknown.

In 2010 Gu et al. (27) identified two enzymes (Supplemented Fig. 2A, B) and their corresponding genes in *Bacillus* food pathogen, and showed their involvement in the sequential conversion of UDP-N-acetyl-glucosamine (UDP-Glc*p*NAc) to UDP-N-acetyl-glucosaminuronic acid (UDP-Glc*p*NAcA), and then to UDP-N-acetyl-xylosamine (UDP-Xyl*p*NAc, UDP-2-deoxy-2-acetoamido-xylose). These enzymes were named UGlcNAcDH for UDP-GlcNAc dehydrogenase and UXylNAcS for UDP-XylNAc synthase. The genes encoding these proteins are located within a conserved six-gene operon (XNAC) that includes, in addition to the nucleotide-sugar biosynthetic enzymes, two genes likely encoding glycosyltransferases and two small proteins of unknown functions. Based on bioinformatics analyses (Supplemented Fig. 2C), the XNAC operon is unique to bacteria of the *Bacillus cereus* group and thus far appears to be lacking in other bacterial phyla. Despite the functional activities of enzymes in the XNAC operon no *Bacillus* glycan composed of GlcNAcA or XylNAc were reported. Hence, it remained unknown if XNAC-genes are expressed and if such glycan is truly made.

Here we provide the first evidence of a glycan that consists of two uncommon amino sugars, GlcNAcA and XylNAc. This glycan, named pzX, is made in *Bacillus* strains belonging to the *B. cereus* group. The formation of this exopolysaccharide occurs when cells are induced to grow in a medium composition known to trigger biofilm formation in *B. subtilis*, and it is released to the extracellular milieu during the release of mature spores.

RESULTS

Growth condition promoting pzX glycan synthesis

Following the finding of genes and the enzymes involved in UDP-GlcNAcA and UDP-XylNAc synthesis (27), the identification of glycan(s) consisting of these unusual amino sugars was unsuccessful when *Bacillus* cells were growing under typical laboratory conditions. We therefore decided to grow *Bacillus* in different growth media in order to find conditions that stimulate transcription of genes in the XNAC operon and promote the synthesis of XylNAc-containing

molecule. RNA isolation followed by RT-PCR analyses concluded that genes likely involved in XylNAc-glycan(s) were not transcribed when *Bacillus* was grown in rich medium like LB or BHI. On the other hand, genes of the XNAC operon were highly transcribed (Fig. 2A) when cells were grown in Msgg, a medium used to induce biofilm formation in *B. subtilis* (28). Under this medium we were able to identify a polymer that contains XylNAc, herein named pzX (fondly for *Z*i's *XylNAc polymer*). pzX was found outside the cells in the culture medium. We found that acidification of the medium led to a selective precipitation of pzX from other components, and such segregation protocol significantly aided in the isolation and further characterization of pzX. Crude pzX obtained from *Bacillus thuringiensis* strain israelensis (Bti) was hydrolyzed by TFA to monosaccharides and derivatized to alditol-acetate prior to separation by GC and analyses by EI-MS (Fig. 2B). Among the neutral monosaccharides residues observed in crude pzX were arabinose (Ara), glucose (Glc) and galactose (Gal) eluting from GC column at 23, 33.5, 34 min, respectively. A peak annotated X (30.6 min) later identified as XylNAc was also observed only when cells were grown in Msgg medium but not in BHI medium (Fig. 2B compare upper and lower panel). A few other amino-sugars residues were observed in the crude pzX including GlcNAc, GalNAc, and ManNAc (not shown). No detectable XylNAc was observed when the *Bacillus thuringiensis* cells were grown in several other rich media including for example LB.

To determine if pzX synthesis is specific to *Bacillus* sp harboring XNAC operon, we examined different *Bacillus* strains grown in Msgg and BHI media. The data (Table 1) show that *Bacillus* strains lacking XNAC operon for instance, *B. megaterium* (Bm) and *B. subtilis* (Bs), did not produce pzX whether grown in Msgg or BHI medium. However, strains harboring XNAC operon like *B. thuringiensis* strain berliner ATCC 10792 (Btb), *B. thuringiensis* strain kurstaki (Btk), *B. thuringiensis* strain israelensis 4Q5 ATCC 35646 (Bti), *B. cereus* ATCC 10876, *B. cereus* ATCC 14579 and *B. anthracis* 34F2, all made pzX glycan but only when cells were grown in Msgg. For reason that remains unclear some strains like Bti, Btb, Btk produce much less pzX-polymer when compared to for example, *B. cereus* ATCC 14579 (Fig. 2C; Table 1). We thus decided to concentrate our effort on elucidating the structure of the pzX from *B. cereus* ATCC 14579 (herein abbreviated pzX ^{bc14579}). Crude pzX ^{bc14579} preparation was bound to anion-exchange column and was eluted with ammonium formate. Alditol acetate analyses of this fraction (Fig. 2D) show predominantly a single neutral monosaccharide, XylNAc. The electron ionization mass spectrometry (EI-MS) of this peak has primary ion fragments (see left insert in Fig. 2D) at *m/z* 288 and 145 along with secondary ion fragments at 246, 228,126, 187, 127 and 103 (right insert in Fig. 2D). The retention time and *m/z* values are identical with those found for alditol acetates derivatives of a XylNAc standard derived from UDP-XylNAc (27). Hence the major neutral sugar in pzX is XylNAc. Since previous works showed that UDP-XylNAc is made by the enzymatic actions of Bc0487 and Bc0488 (27), we addressed if the putative glycosyltransferase (Bc0486) that co-resides in the operon facilitates pzX formation. To this end, we generated Bc0486 mutant (*Δbc0486*) and complemented strains. GC-MS analysis of glycosyltransferase deletion strain (*Δbc0489)* strain reveals no production of pzX in *B. cereus* (Fig. 2E middle panel) while the complementation strain does (Fig. 2E lower panel).

NMR Analysis of pzX ^{bc14579} reveals a trisaccharide repeating units of [XylpNAc(4OAc) α-1,3 GlcpNAcA(4OAc) α-1,3 XylpNAc]n

To gain initial insight into carbon flux leading to pzX and follow the metabolism of glycerol to pzX we fed culture with either a ^{13}C–labeled glycerol at carbon-2 [C2-^{13}C] or at all three carbons [^{13}C3]. Feeding *B. cereus* ATCC 14579 grown in Msgg/[C2-^{13}C]glycerol, where the carbon source glycerol was replaced with glycerol labeled at C2 with ^{13}C, was shown to incorporate the heavy carbon into C2 and C5 position of the XylNAc residue (see left insert in Fig. 2F of non-deuterated alditol acetate XylNAc derivative). The ^{13}C labeling was also incorporated to monosaccharaide residues of other glycans at carbon 2 (C2) and carbon 5 (C5) like hexoses (Glc, Man, Gal), HexNAc's (GlcNAc, ManNAc, GalNAc), pentose (ribose) and 6-deoxy-hexose (Rha). Feeding the

culture with all labeled glycerol (i.e [^{13}C3]glycerol) yielded cells with fully labeled sugars in the six carbon of hexose and 6-deoxy-hexose and the five carbon pentose. The ^{13}C-labeled pzX was purified and used subsequently to determine its structure by NMR.

Our studies shown below will provide evidence that the proposed structure of pzX (Fig. 3A) is a glycan composed of a repeating trisaccharide unit made of three sugar residues that are linked α-1,3 one to another. For the purposes of NMR assignment and description of the pzX glycan we labeled the repeating three sugar residues as A, B and C: **A** refers to XylNAc-4-O-acetate (XylNAc-4OAc), **B** refers to XylNAc residues, and **C** to GlcNAcA-4-O-acetate (GlcNAcA-4OAc). The structure of pzX fits with our current knowledge and genes within the XNAC operon, where the UDP-GlcNAcA is the precursor for UDP-XylNAc (27) and the two glycosyltransferases likely utilize these nucleotide-sugars for the assembly of GlcNAcA and XylNAc into pzX.

pzX ^{bc14579} *consists of three sugar residues*

Initial analyses of purified pzX ^{bc14579} by NMR gave broad peak widths likely due to the high molecular weight and viscosity of this molecule. To reduce the size and obtain sharper spectra, pzX ^{bc14579} was sonicated and NMR analysis was carried out at 65 ^{o}C. One-dimensional ^{1}H-NMR revealed three clear regions (Fig. 3B) each consists of overlapping proton peaks: Protons (5.05-5.26 ppm) belonging to the sugar anomeric region (H-1) together with downfield shifted protons (H-4s) that derived from O-acetylation (see discussion below); the resonances of sugar ring protons between 3.2 and 4.2 ppm; and proton signals between 1.9 and 2.2 ppm of terminal methyl group protons (typically found within acetate moiety). One-dimensional ^{13}C NMR of ^{13}C fully labeled pzX ^{bc14579} gave four distinct spectral regions that are consistent with the structure: the anomeric carbon region (~100 ppm) shows three major glycosyl residues (Fig. 3C, see boxed window), each showing expected doublet peak as a result of anomeric peak split by ^{13}C labeled carbon-2 of pzX ^{bc14579}. The three other regions of the ^{13}C-spectrum show several resonances near ~175 ppm, near ~23 ppm and several signals between 80-50 ppm, each fits to the chemical shifts of the carbonyl (C=O), the methyl (CH_3) groups of acetate, and the carbons from the sugar ring, respectively. To complete the assignment of sugar residues and confirm the structure of pzX ^{bc14579}, two-dimensional NMR including COSY, TOCSY, NOESY, HMQC, HSQC, HMBC, HMQC-TOCSY and HMQC-NOESY were acquired. The complete chemical shifts assignments of pzX ^{bc14579} and of de-O-acetylated form of pzX ^{bc14579} are provided in Table 2 and Table 3, respectively.

pzX ^{bc14579} *sugar residues A, B are identified as 2-deoxy-2-N-acetyl-xylose*

The initial carbon-proton correlated two-dimensional NMR signals were not prominent and gave poor signal intensity. This problem was overcome after generating *in vivo* pzX ^{bc14579} samples that were ^{13}C-labeled. pzX ^{bc14579} was either selectively ^{13}C-labeled in carbons 2 and 5 or fully ^{13}C -labeled in all carbons. This labeling was obtained by purifying pzX ^{bc14579} from *B. cereus* cell fed with glycerol[C2-^{13}C], or fully labeled ^{13}C-glycerol, respectively.

Two-dimensional HMQC analyses show the protons directly bonded to their carbons. Analyses of the [2, 5 ^{13}C]pzX ^{bc14579} sample show three C5/H5 signals (Fig. 4A) as well as a number of C2/H2 signals (Fig. 4B). The three C-5/H-5 signals have carbon chemical shifts between 60 and 75 ppm. The C-2/H-2 signals (A, B, C) have noticeably upfield carbon chemical shift (~54 ppm) and downfield proton (H-2) chemical shifts around 4 ppm. These three upfield carbon chemical shifts are consistent with a nitrogen attached to carbon 2. The downfield proton chemical shifts suggest that the C-2 nitrogen is acetylated; i.e. C-2 is attached to an N-acetyl group. Taken together, each of the three A, B, C residues contains a carbon C-2 that has an N-acetyl substituent; i.e. all three residues are C-2 N-acetylglycoses. Panel A (Fig. 4) also shows that the C-5 carbons of residues A and B each has two attached protons indicating that both residue A and B are pentoses. Analyses of de-O-acetylated pzX ^{bc14579} sample (see below) strongly support that the C5-pentose ring for both residue A and B is in a *xylo*-configuration based the large (~10-11) J coupling constant between H4 and H5b (Table 3). Hence, the NMR data indicate that A

and B are XylNAc (2-deoxy-2-N-acetyl-xylose) which is in agreement with the GC-MS data (Fig. 2D).

pzX ^{bc14579} *sugar residues C is identified as 2-deoxy-2-N-acetyl-glucuronic acid*

The C-5/H-5 signal in HMQC spectra (Fig. 4A) for residue C shows its carbon is linked to a single proton implying that C-5 is bonded to another nuclei. Four lines of experimental evidence provide support that residue C is N-acetyl-glucosaminuronic acid (GlcNAcA) residue. The first proof was obtained by a ^{13}C carbon-carbon connection INADEQUATE experiment (Fig. 4D) with ^{13}C fully labeled pzX ^{bc14579}, [^{13}C]pzX. INADEQUATE experiment shows a pair of signals for C-5 of and a C-6 carbon with chemical shift of 176.4 ppm that fits resonance of CO likely a carboxylate (COO^-) group (Table 2). This data along with C2/H2 HMQC established that C is a N-acetylhexaminouronic residue. The subsequent multiplicity-edited HSQC NMR experiment (Fig. 4E) illustrated the C-5/H-5 groups of residue A and B have different phase (blue) indicating that these carbons are linked to two hydrogens, as expected for XylNAc sugar residue. On the other hand, C-5/H-5 group of residue C has opposite phase (red) supporting the INADEQUATE and HMQC experiments that showing that its C-5 carbon is bonded to a single hydrogen as well as to C-4 and C-6. The HMBC spectrum of the de-O-acetylated sample (Fig. 4F) also shows that residue C has cross-peaks from C-6 to H-4 and to H-5 consistent with it being a N-acetylhexaminouronic residue. To determine if residue C is in *gluco*- or *galacto*- configuration, pzX was TFA-hydrolyzed; and sample was analyzed by TOCSY. As expected, the acetate of OAc and NAc groups were cleaved upon the acid treatment to yield an amino monosaccharide (i.e. 2-deoxy-2-amino-hexouronic acid), of which the large coupling constants of $J_{4,5}$=8.3, $J_{2,3}$=9.4, $J_{3,4}$=8.2 Hz are consisted for residue with *gluco*-configuration and the small coupling of $J_{1,2}$=3.6 Hz supports an alpha sugar. Hence, the NMR data along with sugar analyses by HPLC (Fig. 4G) indicate that residue C is GlcNAcA (i.e. N-acetyl-glucosaminuronic acid). Further analysis of HMQC-TOCSY spectra of the partially ^{13}C-labeled pzX ^{bc14579} provided additional chemical shifts (see Table 2) that are consistent with GlcNAcA.

Residues A and C of pzX ^{bc14579} *are 4-O-acetylated*.

The unusual higher than expected downfield chemical shifts of H-4s (~5 ppm) in residues A and C (Fig. 4 C, E) imply a substitution at position 4 of those residues. The carbon and proton C-4/H-4 in both residue A and C have increased C/H chemical shifts of ~ 75/5 ppm (Fig. 4C,E) consistent with O-acetylation when compared to unacetylated C-4 with C/H shifts of ~70/3.7 ppm. The correlation between H4 and a carbonyl carbon in the HMBC of the partially ^{13}C-labeled [C2, C5 ^{13}C] pzX ^{bc14579} further confirmed that the substitution on the C-4 position of residue A and C is *O*-acetate (Fig. 5 panel A). The carbons from the carbonyl region (~175 ppm) show cross peaks to proton H-4 in both residue A and C (Fig. 5A on the left side). Additional cross peak from the same carbonyl carbon to the methyl hydrogens (panel A on the right side) indicates that an acetate group is attached to carbon C-4 of residue A and C. Hence, residue A is XylNAc-4-O-acetate (XylNAc-4OAc) and residue C is GlcNAcA-4OAc. Further support for 4-OAc bonded to C-4 in residue A and C is shown after chemical hydrolysis of the ester group.

The ester linkage of O-acetate (C-4-OAc) group should be more susceptible to de-acetylation when compared with the amide N-linked acetate (C-2-NAc). Hence, base treatment of pzX ^{bc14579} should remove the O-acetate group from C-4 but keep the N-acetate linked to C-2 intact. Indeed, HSQC NMR analysis of the de-O-acetylated pzX ^{bc14579} sample shows that the original signals for C-4/H-4 protons of residues A and C (Fig. 4E) were shifted to the more conventional position with chemical shifts around 3.8 ppm (marked by arrow in Fig. 5 panel B). Comparison of one-dimensional proton NMR between before and after de-O-acetylation (Fig. 5C) also indicates a significant reduction in intensity of the methyl group region (dotted boxes) of the O-Ac group. As expected, no obvious shift in the protons linked to C-2 regions of A, B, and C residues (Fig. 5B, C-2/H-2 ~55/~4 ppm) is consistent with the expectation that the C-2-*N*-acetate groups are untouched after KOH treatment.

Residue A, B, and C are alpha 1-3 linked to each other.

The position of the glycosidic linkages was determined initially by per-O-methylation analysis using GC-MS (Fig. 6 A, B). The free hydroxyl groups of intact pzX ^{bc14579} were methylated and the per-O-methylated glycan was hydrolyzed. The resulting monosaccharides were reduced, acetylated, and the partially methylated alditol acetates (PMAA) were separated by GC-MS. A single peak eluting at 27.3 min gave primary and secondary ion fragments (Fig. 6B) with the following *m/z* values: 274, 231, 229, 171, 159 and 117. The *m/z* 159 and 117 ion fragments are diagnostic for NAc group attached to carbon 2 of the sugar residue, and the ion fragments 171 and 231 along with the other *m/z* values indicates this peak is a 3-O-acetyl-4-O-methyl-2-methyl-2-acetoamido-2-deoxy-xylitol. These PMAA analyses support that XylNAc residues on pzX ^{bc14579} are 1-3 linked, however, linkage information related to the acidic residue C, GlcNAcA was not provided. Thus, further NMR experiments were conducted to complete the linkage analyses.

The linkage positions between the sugar residues were confirmed using HMBC and HSQC-NOESY spectra (see Fig. 6C, D, and E). In NOESY, if sugar residues were connected in α-configuration one would expect a strong NOE from H1 to H2 (for both XylNAc and GlcNAc configuration) because both proton are facing up and close in proximity. In the TOCSY spectrum however, one would expect for α-configuration to have a weak cross peak between H1 to H2, but a very strong cross peak in ß-linked sugar residues. HSQC-NOESY spectrum of de-O-acetylated pzX shows strong NOEs between H1 and H2 within the same sugar residue (Fig. 6C), whereas weak cross peaks between H1 and H2 were detected in the HSQC-TOCSY spectrum (data not shown) suggesting both protons are close in proximity but with small coupling, thus each sugar residue are in α-configuration. The HSQC-NOESY experiment shows additional cross peaks between H-1 of residue A and H-3 of residue C (Fig. 6D) indicating residue A and C are 1-3 linked (**a**C1-**c**H3) (Fig. 6D). Similarly, residue B and A, and residue C and B are 1-3 linked due to inter-glycosidic cross peaks between C-1 and H-3 (**c**C1-**b**H3; **b**C1-**a**H3). The same combinations of inter-glycosidic cross peaks were detected in HMBC experiment (Fig. 6E). Both spectra together with PMAA analyses support the fact that sugar residues A, C and B are linked A(1-3)C(1-3)B. *In toto* the NMR data provide strong evidence for the sugar sequence and configurations of the glycosidic linkages of pzX^{bc14579} glycan to be → XylNAc4OAc(α 1 → 3)GlcNAcA4OAc(α 1 → 3)XylNAc(α 1 →.

pzX isolated from Bacillus anthracis Sterne 34F2 and B. cereus ATCC 10876 is similar to pzX^{14579}

Initial GC-MS analyses of crude pzX isolated from the medium of Msgg-grown *B. anthracis* and *B. cereus* 10876 showed predominantly the XylNAc residue (Fig. 7 panel A). Further purification and analyses by proton-NMR (Fig. 7B) and TOCSY 2D-NMR (Fig. 7C) provided evidence that the purified EPS from the *B. cereus* ATCC 10876 and *B. anthracis* 34F2 have similar structures to the pzX from *B. cereus* ATCC 14579. The *B. anthracis* 34F2 strain used in this study is the one isolated by Max Sterne in the 1930's, the strain that was used to develop vaccine to anthrax in animals (2). The conserved chemical structure among the pzX from these *Bacilli* characterized in this report thus far suggests that it has a common role that is shared by all members of the *B. cereus* group.

pzX is synthesized during late stationary growth phase and released into extracellular milieu

In order to address the timing of pzX^{bc14579} synthesis and determine if it is further metabolized, we monitored the amount of pzX daily for 14 days in cells grown in Msgg medium. pzX^{bc14579} starts to accumulate around the second day, with highest amounts being produced during day 4-to 6 to a level of approximately 10 µg/ ml culture. Between days 6 to 14 in the culture, no further accumulation or degradation of pzX was observed, suggesting it is not catabolized. Microscopy analyses (Fig. 8A) show that once cells shifted to grow on Msgg, vegetative cells continued to grow and replicate (8 h). Between 12 h to 24 h, at which point cell density of 3 was reached, the cells entered aggregation phase and asynchronous sporulation, which consisted of mixed cell types

with less than 10% spores. At 48 h, maximum cell density was reached (OD_{600}, 5.5), and the cells entered the beginning of de-aggregation phase and started to release ~20% mature spores. At day 3 as cell aggregation continued to disintegrate, the OD was reduced to 4.8 as more mother cell lysed during sporulation. And on day 4-6 almost all cells (>90%) in the culture completed sporulation and released dormant heat stable spores as confirmed by the ability of cell survival after 80 ^{o}C (Fig. 8B). The pattern of $pzX^{bc14579}$ accumulation overlays with the release of spores into extracellular milieu when cultures are grown in Msgg (Fig. 8B). pzX formation was not detected when cells were grown in rich medium that does not support sporulation like BHI, not even after 14 days in culture.

The timeline of $pzX^{bc14579}$ formation was further studied using different media known to enhance biofilm or sporulation of *Bacillus* sp. All media at day 1 produced cell aggregates. This was followed by de-aggregation phase and mature spore release after 5 days similar to Msgg medium. The media tested (Fig. 8C) included CDS-Glc, G, modified Tempest, CDM, DSM, EPS, and HCT, all produced pzX as determined by GC-MS analyses albeit in different amounts. Interestingly, rich medium DSM, which is known to support spore formation, produced much smaller amounts of $pzX^{bc14579}$ compared to Msgg. This finding along with the previous observation that rich media like BHI, LB, and TSB prevent $pzX^{bc14579}$ formation prompted us to test if rich medium suppresses pzX synthesis. We examined cultures grown in Msgg (control) and cultures grown in Msgg supplemented with various amounts of rich medium components. GC-MS analyses of crude $pzX^{bc14579}$ (Fig. 8D**)** showed that moderate increased addition of nutrient broth (comprised of beef extract and peptone), tryptone and low glucose to Msgg culture broth do affect the amount of pzX. However the addition of excessive dosage of rich medium (e.g. 8 g/L nutrient broth or 5 g/L tryptone), that is comparable in amounts to DSM or HCT medium, or high level of glucose (3%) prevents the formation of both pzX and spores. Collectively, the data suggest that pzX is released to extracellular milieu predominantly when spores are made. It appears that the production of pzX is regulated by several factors that include the type and amount of nutrients (e.g. glucose), the environment (where more pzX is made in shaking vs. still cultures), and lastly the completion of sporulation.

pzX has surfactant, adherence and antiaggregant properties

Further investigation into the role of pzX in the extracellular medium revealed that pzX has a surfactant property with the ability to increase the growth diameter of a colony when grown in agar by over 30% (Fig. 9A). The surfactant property was determined by the drop collapse method, and the data show that when pzX is dissolved in deionized water it decreases the surface tension of water from 84 to 34^{o} (Fig. 9B). The dose response curves show that the surface tension decreases continuously with increasing concentration of pzX. The decrease in surface tension is not affected if pzX is deacetylated or autoclaved (Fig. 9C) suggesting that the glycan is heat stable and maintains its property even under alkaline or hydrolytic conditions that may strip off its O-acetate side-chain decoration. We also observed surfactant activity with *B. subtilis* suggesting that this property of the glycan is not unique to *Bacillus cereus* sensu lato group.

Since no apparent degradation of $pzX^{bc14579}$ is observed after spores are released, we investigated the role of pzX as a molecule that increases/decreases adherence of the spores to surfaces. Figure 10 panel A left shows that in the presence of pzX 56% of spores adhered to the surface of a defined soil-like material (vermiculite) when compared with control showing 16% of adherence. The adherence to vermiculite is dose-dependent (Fig. 10A right), suggesting that with increasing amount of pzX in the extracellular milieu of the spores, a higher number of cells will adhere to environmental surfaces.

To investigate the role of pzX after spore germination we carried out the following experiments. First we determined that pzX itself is unable to induce spore germination (data not shown). To examine pzX post spore germination we incubated germinated *Bacillus* spores with no nutrient for 2 days in the presence or absence of pzX. The phase-contrast microscopy analyses (Fig. 10B) suggest that germinated *B. anthracis* spores

tend to aggregate, however, pzX reduces aggregation (antiaggregant). The CFU counts (Fig. 10C) show a decrease during the first 4 hours, indicating an initial aggregation immediately post germination. However, post the 4 hours window, the CFU count is increased to its initial level, likely due to the antiaggregant activity of pzX.

Since the chemical and physical property of pzX is to precipitate below certain pH, and the data so far suggest that pzX co-forms with spores, we wonder how spores behave at such environment. To test this, *Bacillus anthracis* spores were challenged with pH 2 for 24 h in the presence or absence of pzX. Spores without pzX aggregate and settle to the bottom (Fig. 10D) as expected. However, we were surprised to notice that the spores with pzX formed a cotton fluff-like structure that floated on the top of the culture (see Fig. 10D bracket labeled UP). Analyses of spores above or below the floated fluff show that the cotton structure consists a significant number of spores (Fig. 10E). Phase-contrast microscopic analyses (Fig. 10F) reveal that the fluff-pzX forms a film-like structure that harbors the spores. Interestingly in such matrix configuration, the spores do not aggregate (see Fig. 10G).

DISCUSSION

Bacterial pathogenic species belonging to *Bacillus cereus* group have an advantage in nature due to their capacity to survive for many years as dormant spores despite harsh changes in the environment. Past work utilized purified spores to examine their chemical and physical properties in adaption and fitness to environment or to examine infection processes, but here we provide new evidence that dormant spores are in fact, co-made within an extracellular matrix containing an unusual polysaccharide, pzX.

The XNAC operon consists of two nucleotide-sugar biosynthetic enzymes that were biochemically shown to form the precursors UDP-GlcNAcA and UDP-XylNAc (27), and two glycosyltransferases that are likely involved in pzX synthesis. Genomic data (Fig. 1C) reveal that all strains belonging to this group carry the XNAC operon in their chromosomes and therefore have the capacity to synthesize pzX. We further examined this capacity by analyzing six random *Bacillus* members of this group representing strains from different phylogenetic clades (see * in Fig. 1C), and showed they all produced pzX, while non-group members like *B. megaterium* or *B. subtilis* that are lacking the XNAC operon in their chromosome did not produce pzX (Table 1). The collective biochemical analyses including ^{13}C-carbon labeling, sugar methylation, GC-MS and NMR analyses provide strong evidences that pzX backbone consists of a repeating trisaccharide sequence of [-*3*)XylNAc(*α1-3*)GlcNAcA(*α1-3*)XylNAc(*α1*-]$_n$ and with a side chain decoration of O-acetate group link to C-4 of XylNAc and to C-4 of its acidic amino sugar, GlcNAcA. Hence, the chemical structure of pzX agrees with the two UDP-sugar biosynthetic enzymes encoded by the XNAC operon (Fig. 1A). Taken together, the conserved pzX chemical structure among the three *Bacillus* strains (*B.* cereus ATCC 10876, *B. cereus* ATCC 14579, *B. anthracis* Sterne 34F2) as characterized by NMR (Fig. 7) and the conserved XNAC operon let us to propose that pzX has a common role that is shared by all members of the *B. cereus* group.

In addition to biochemical analyses, we have shown that the XNAC operon is directly involved in pzX formation in members of the *Bacillus cereus* sensu lato. For example, deletion of the glycosyltransferase (*Δbc0486*) yielded no pzX (Fig. 2E) in *B. cereus* ATCC 14579. Similarly deletion of glycosyltransferases in *B. thuringiensis israelensis* (Bti) strain also showed no production of pzX (data not shown). This genetic data provide strong evidence that the glycosyltransferase encoded by XNAC operon is involved in the synthesis of pzX.

Although *Bacillus* pathogens have been studied extensively for many years, it is not surprising that pzX was not detected since typical laboratory growth media is discarded during spore isolation, and specific and extensive analytical methodology will be required to identify, purify and characterize minute polysaccharides. pzX is formed when *Bacillus* cells are grown in a defined nutrient medium, like Msgg, however, other media also support its formation (see Fig. 8C). The data so far suggest that pzX is accumulated during sporulation, however, the relative amount may be regulated by the amount of nutrient available. For

example, when the defined medium Msgg was supplemented with 0.5% glucose, higher amount of pzX was produced in comparison to cells grown in Msgg alone. Higher amount of pzX can also be made when Msgg is supplemented with small amount of undefined medium (see Fig. 8D). Other defined nutrient media differing in composition that support sporulation also support pzX formation (Fig. 8C). On the contrary, media that do not support sporulation produce no pzX. For instance, pzX was not detected when strains were grown in rich medium (like BHI and LB) even after prolonged time (2-6 days of incubation) or when Msgg was supplemented with a rich medium component or with 3% glucose, as those media did not support mature spore formations (Fig. 8D). Analyses of the putative promoter DNA region, 5' to Bc0484, revealed sequences that potentially can be recognized by the sporulation specific sigma factors, SigG and SigE. Clearly, future studies will be required to identify the molecular mechanism that controls pzX formation.

Interestingly, little pzX was observed when *B. cereus* ATCC 14579 were grown in Difco Sporulation medium (DSM). This observation raises two questions: do all sporulation media make identical spores or are some spores made in certain medium chemically or physically different from others? Since DSM has excessive nutrients that probably do not mimic natural environments *Bacillus* would encounter, we propose that under natural settings spores are made with pzX. Alternatively, DSM may consist of a factor that suppresses pzX formation. We are currently pursuing a study aimed at identification of nutrient factors controlling XNAC operon gene expression, the accumulation of intermediate metabolites, and the amounts of pzX formed. Further studies are clearly needed to elucidate the molecular mechanism that senses, controls and regulates the level of pzX accumulation. The relationship between nutrients and pzX may identify new regulatory factors that tune (enhance or suppress) the flux of metabolism to pzX formation, and factors that control EPS common to only species belonging to *B. cereus* sensu lato group.

The biological role of pzX as biosurfactant (see Fig. 9) is complex. Some surfactants are toxic, but we have seen no such toxic effects of few laboratory *E. coli* and fungal strains that were co-cultivated on agar with pzX. The surfactant could enhance the spread of germinated spores and this may give an advantage over other bacteria fighting for limited nutrient resources. We have shown that pzX precipitates at low pH, most likely due to protonation of its acidic sugar GlcNAcA. The precipitated pzX is dissolved when pH is higher than 4-5. While several factors are known to protect the spore including for example, spore outer coat layer and the exosporium (29), we cannot exclude the possibility that glycan (pzX) is an additional factor in spore biology. It is therefore probable that under acidic environments (e.g. human stomach, soil) precipitated film pzX like-structure (Fig. 10F) gives additional protection to the spore. Contrary to animal, the midgut cavity of some larvae is alkali and under such high pH, pzX is not degraded. Despite the fact that the O-acetate could be cleaved under alkali condition, our data show that the biosurfactant property is still maintained even when pzX is de-acetylated.

The pzX adherence assays (Fig. 10A) show that spores mixed with pzX adhere significantly stronger to an artificial soil surface (vermiculite) in comparison to spores alone. This is difficult to interpret, and our current working model is that pzX enclosed and trapped spores to the soil surface during desiccation. Brief contact with water may not be sufficient to re-hydrate pzX and release spores. This adhesion property may have a more profound affect under acidic soil environment where larger amounts of dormant spores may cling to a soil particle rather than being washed away. Further research will be required to determine if pzX adherence property plays a role during interaction or persistence with the microbial host.

Following sporulation we found no evidence that pzX undergoes hydrolysis despite the fact that the mother cell releases many hydrolytic enzymes. Furthermore, the chemical nature of pzX and its distinctive α-1,3-linked amino-sugars suggest that it may protect cells from common lytic enzymes like lysozyme, an enzyme that cleaves β-1,4-linked sugars. Taken together, the results of the present study reveal a novel extracellular polysaccharide that is formed during sporulation and likely to play multiple roles in the interaction

of the spore with its environment. Many questions still await answers to fully understand the biology of this novel polysaccharide we named pzX.

EXPERIMENTAL PROCEDURES

The bacteria used in this study (Table 1) were stored in BHI containing 16% glycerol at -80 °C. *Bacillus* strains were routinely grown in BHI medium, LB, or Msgg medium (28). In addition, various sporulation and biofilm-inducing media were used: CDS-Glc (30), EPS (31), HCT (32), modified Tempest medium (33) with 5 mM phosphate and 0.1% glucose, modified-G medium (34), the modified Schaeffer (35) also known as Difco sporulation media (DSM), and CDM medium (36). Spores were separated from medium of 5 days culture by centrifugation (8,000 g, 10 min); washed with sterile deionized water (ddw), suspended and pelleted again before storage (up to 1 month) to give a total yield of 10^9 per ml. The number of spores in liquid culture was determined after heat treatment at 80 ^{o}C; conditions that activate spores and kill any remnant vegetative cells (37). An aliquot of a culture was heat-treated for 20 min at 80 °C, cooled to 25 °C and vortexed, and serial dilutions were plated on BHI-1.5% agar plates. Total CFUs and the percentage of spores from vegetative cells were estimated by comparing samples that were heat and non-heat treated.

RNA isolation and RT-PCR

B. thuringiensis cells were grown in different liquid media (e.g. BHI, LB, Msgg) to an OD_{600} of 4-5.5; and cell amounts equivalent to OD_{600} of 4 were pelleted at 6,000 g for 1 min at 4 °C, resuspended in 800 µl of lysozyme solution (10 mM Tris-HCl pH 8, 1 mM EDTA, 10 mg/ml lysozyme), and incubated at room temperature for 10 min. Each sample was supplemented with 80 µl 10xEB (0.3 M NaOAc pH 5.2, 50 mM EDTA, 5% sarkosyl and 1.42 M β-mercaptoethanol), and incubated at 65 °C for 2 min, followed by addition of 1 volume of one-phase 70 °C preheated acidic phenol (phenol:AcE buffer (50 mM NaOAc pH 5.1, 5 mM EDTA) 1:1 v/v). After brief vortex and incubation at 65 °C for 7 min, each sample was centrifuged (10,000 g for 5 min at 4 °C); the aqueous layer was collected and mixed with 1 volume of chloroform. Nucleic acid partition to upper phase was collected and precipitated with cold ethanol and 30 mM NaOAc pH 5.2 at -20°C. The concentration of crude RNA was determined from the absorbance at 260 nm. To digest remnant genomic DNA contamination, an aliquot of 5 µg crude RNA was treated with DNase I. The resulting RNA was ethanol-precipitated and about 250 ng of RNA was used for further reverse transcriptase (RT) and PCR reactions. For cDNA synthesis the 20 µl RT reaction was consisted of 250 ng of RNA, 5 µM random hexamers as primer, buffer, 0.2 µM dNTP's and 1 unit of reverse transcriptase (SuperScript III, Invitrogen). Negative control RT reactions were done without added primer. Transcripts of genes in XNAC operon and Sigma A as positive control (sigA, rpoD BC4289) were amplified using a 25 µl PCR reaction that included 2 µl of RT reaction, buffer, dNTPs, 1 unit of Taq DNA polymerase (Fermentas) and 0.4 µM of each gene specific sense and antisense primers (ZL035-5'-ctagcattcatctgtattcttttcttcc; ZL036-5'-gcagatatttgtttattcgttgatggtg; ZL037-5'-tcatacactcaccttctttataattcc; ZL038-5'-atctacaaaaccgtttggatttactc; ZL039-5'-ttagccattgttttcttcatgaaacc; ZL040-5'-cgttattttaatatttatggtccaagagc; ZL041-5'-ctataaaacatctctttttctattgccatc; ZL042-5'-attatttagatctaagagtaccacttcatc; ZL043-5'-ctattctaagaaatccttaagacgcttac; ZL044-5'-caattcgtattccagttcatatggttg). Following PCR, a portion (5 µl) of each RT-PCR reaction was loaded on 1% agarose-TAE gel casted with 10 µg/ml ethidium bromide, separated by gel electrophoresis and UV-imaged using gel imager.

Isolation, purification and analyses of XylNAc-glycan, pzX

A portion of *Bacillus* strain cells grown in BHI (0.5 ml) was used to inoculate 50 ml Msgg medium and culture was incubated for 4 days at 30 °C, shaking at 200 rpm. The culture was centrifuged (10,000 g, 10 min, 4 °C) and the medium was filtered prior to lowering the pH to 2. After centrifugation (8,000 g, 1 h, 4 °C), the precipitated crude pzX polymer was washed; resuspended with deionized water, and the sugar composition was analyzed by GC-MS. For purification, the crude pzX solution was chromatographed on Q-sepharose (GE, 5 ml column) pre-equilibrated with 5 mM ammonium formate, and eluted by stepwise gradient of increasing concentration of ammonium formate.

The purified pzX eluted at 400 mM ammonium formate was lyophilized, dialyzed against deionized water, and used for further analyses. To obtain ^{13}C-labeled glycans, the glycerol in Msgg medium was substituted with carbon-2 labeled glycerol, [C2-^{13}C]glycerol, or with uniformly labeled glycerol, [^{13}C3]glycerol (Cambridge Isotope laboratories). Following 4 days of incubation, cultures were processed and pzX was purified as above. The size of pzX was determined by gel filtration on Superdex 75 column (1 cm i.d. x 30 cm, GE). An aliquot of pzX (0.5 ml) was injected via Agilent HPLC system equipped with UV detector (200 nm) to the column and chromatography was carried out at a flow rate of 0.5 ml/min using 0.5 M NH_4HCO_3.

To determine neutral and amino-sugar composition of crude pzX, column fractions, or purified pzX glycan, an aliquot was supplemented with 10 µg inositol; hydrolyzed with 2M trifluoroacetic acid (TFA) at 120 °C; and the released monosaccharides were reduced to their alditols (38), and acetylated. The resulting alditol acetate derivatives were analyzed by GC/EI-MS system (Agilent 7890a/5975c), equipped with an autosampler injector (Agilent 7693). A 1 µl sample was injected into GC-column (Equity-1 or DB-5, 30 m × 0.25 mm, 0.25 µm film thickness) using split mode (1:50) with injector inlet setting of 250 ^{o}C (helium at 3 ml/min). Helium was also used as column carrier gas (1 ml/min). After injection, the GC column chamber temperature program was held for 2 min at 80 ^{o}C; the temperature was increased to 140 ^{o}C at a rate of 20 °C/min, followed by an increase to 200 ^{o}C at 2 ^{o}C/min; an increase to 250 ^{o}C at 30 ^{o}C/min; finally the temperature was held at 300 ^{o}C for 5 min before next sample injection (run time of ~ 50 min). The MS detector was operating under electron impact (EI) ionization at 70 eV and the temperature of the transfer line between the column end to MS was 250 °C. The temperature of the MS source was 230 ^{o}C and the quadrupole 150 ^{o}C, respectively. MS data were collected after solvent delay of 5 min, in a continuous scanning mode, recording ion abundance in the range of 50-550 m/z. The spectra were analyzed using Software MSD ChemStation D.02.00.275 (Agilent Technologies). To determine the elution time of authentic XylNAc and the EI-mass fragments formed, UDP-XylNAc was produced enzymatically and purified over Q15-column (27); TFA-hydrolyzed, converted to alditol-acetate, separated by GC using DB-5 column and analyzed EI-MS using above GC conditions.

O-Methylation, de-O-acetylation, and HPLC-PAD analyses

The position of glycosidic linkages was determined by methylation analysis. Dry pzX-glycan was dissolved in 200 µl dimethylsulfoxide and free OH groups were methylated with methyl iodide in a NaOH-DMSO slurry as catalyst (39) for 7 min at room temperature; the resulting per-O-methylated pzX was extracted with dichloromethane and dried. The O-methylated glycan sample was TFA-hydrolyzed, and the released partially methylated monosaccharides were reduced with $NaBD_4$; acetylated with acetic anhydride in pyridine and the derived partially methylated alditol-acetate derivatives were analyzed by GC-MS as described above. For MALDI-TOF MS analyses, 1 µl of per-O-methylated-pzX oligosaccharides was mixed with 1 µl DHBA solvent (10 mg α-dihydroxybenzoic acid in 0.5 ml MeOH:H2O v/v) and spotted on MALDI plate and mass spectrometry was carried out in positive mode (Bruker microflex LT MALDI-TOF). To obtain pzX glycan lacking O-acetate groups, purified pzX glycan was incubated for 2 h with 1M KOH at room temperature, dialyzed three times against 2 liter of deionized water, lyophilized and resuspended in D_2O for NMR analyses. For HPLC analysis of pzX sugars, purified pzX was hydrolyzed by 2 M TFA at 120 °C for 2 h, and the excessive TFA was evaporated by air flow followed by three times of 1 ml 2-propanol washes. Samples were dissolved in 100 µl of water, and 10 µl of each was separated by Dionex-Carbopac PA1 column and detected by PAD.

Characterization of pzX by NMR

For NMR analyses, approximately 1 mg of the Q-column purified pzX fraction was desalted by dialysis (1k MWCO), sonicated at amplitude of 45 (S-4000 Misonix Inc, Farmingdale, NY) fitted with a 1/8-inch microtip probe) for 80 cycles each of 30 sec pulse, 30 sec rest, dried by Speed-Vac,

and dissolved in 200 µl of D2O (99.99% deuterium) supplemented with 1 µl of 10 mM DSS (4,4-dimethyl-4-silapentane-1-sulfonic acid). The sample was centrifuged and transferred to a 3-mm NMR tube and NMR data were recorded at 65 ^{o}C on an Agilent DD2 600 MHz NMR spectrometer equipped with a cryogenic 3 mm probe. Standard pulse sequences were used unless otherwise mentioned. Proton and carbon chemical shifts were referenced to an internal DSS peak set at 0.00 ppm for both proton and carbon spectra. The structure of pzX glycan was analyzed using one- and two-dimensional proton and carbon NMR experiments. The one-dimensional (1D) proton NMR spectrum was recorded using the water-presaturated pulse sequence and obtained with a spectral width of 6 kHz, a 90° pulse field angle (7.5 μs), a 2.7-sec acquisition time, and a 2-sec relaxation delay (RD). The free induction decays (FIDs) were multiplied by an exponential function with a line-broadening factor of 1.5 Hz before Fourier transformation. The one-dimensional ^{13}C spectra were obtained with a spectral width of 37.9 kHz, a 45° pulse field angle (7.5 μs), a 0.87-sec acquisition time, and a 1-sec relaxation delay (RD). The free induction decays (FIDs) were multiplied by an exponential function with a line-broadening factor of 3 Hz before Fourier transformation. In addition to ^{1}H and ^{13}C 1D NMR spectra, a series of homo- and heteronuclear two-dimensional NMR data sets were obtained including HMQC, HSQC, HMBC, INADEQUATE, and HMQC-TOCSY, HMQC-NOESY, HSQC-NOESY. Each experiment was modified to accommodate optimal setup to detect complex glycan structures. One-bond coupling constant was set to 170 Hz and the two-dimensional data were processed using Gaussian functions and zero-filled to a final size of 2000 × 1000. Data processing and plotting were performed using software MestreNova.

XNAC operon Mutants

Gene knockout was achieved by double crossover recombination that designed to replace large middle portion of the target gene with chloramphenicol resistance and mKate2 cassette. Two DNA fragments flanking bc0486 gene from *B. cereus* ATCC 14579 were PCR amplified by primer sets ZL009: 5'- ggatccgatatcgcccgacgcgaggctggatggc -3'; ZL123 5' –gaattcgatccttatctgtgcccca gtttgctagg-3' and ZL405 5'- cagataaggatcgaattctgattcgggaaataaagtaagc -3'; ZL406 5'-ggcgatatcggatccctaatgcgtgggctgcatcttc-3' and they were individually cloned into pZL accepting shuttle plasmid, a derivative of pBCB13 (40) that harbors the thermosensitive ori from pMAD (41) and facilitates a cloning strategy for chromosomal integration at non-permissive temperature and subsequently a double crossover recombination event. The resulting pZL-KO-bc0486 plasmid was transformed to *E. coli* strain INV110 (Dam^{-}; Dcm^{-}, Invitrogen) to isolate unmethylated plasmid followed by electroporation (42) into wild type *B. cereus* ATCC 14579 competent cells. The double recombinant mutant strains were screened for chloramphenicol (5 µg/ml) resistant and erythromycin (5 µg/ml) sensitive clones and the positive *Δbc0486* was further confirmed by PCR screen to validate independent double crossover events. For *Δbc0486* complementation, a 1.5 kb fragment containing the Bc0486 homolog from *B. thuringiensis israelensis* ATCC 35646 was amplified by PCR and cloned by in-fusion into pDZ vector, a derivative *E.coli/Bacillus* shuttle plasmid of pDG148-stu (43). The resulting construct carrying constitutively expressed promoter Phspank, functional glycosyltransferase gene and kanamycin resistance gene and was then electro-transformed into *Δbc0486* as previously described. Positive clones were selected on TSA plates supplemented with 5 µg/ml kanamycin.

Surfactant analysis of pzX

To study the effect of pzX on the growth of *Bacillus*, purified native pzX, de-O-acetylated pzX or autoclaved pzX derived from 100 ml Msgg culture of *B. cereus* was dissolved in 1 ml of sterile deionized water (DDW) and 50 µl was plated on half of Msgg (1.5% agar) plate, while 50 µl of sterile DDW was plated on the other half as control. A 2 µl drop of vegetative cells or spores prepared from 8 h BHI or 4 days BHI culture, respectively, was spotted on both halves of the plate and the plate was incubated inverted at 30 °C for 2 days. An aliquot of 50 µl 0.1% SDS was also layered on half of Msgg agar plate as positive control. Pictures were taken by both handheld microscope and dissecting microscope. To measure the surface tension of water in the presence or absence of purified native pzX, de-O-

acetylated pzX or autoclaved pzX, a square area of 1.2 cm^2 of flat polystyrene surface was spread with either 10 µl of DDW or each of the pzX samples, and the liquid was allowed to dry. Various amounts of DDW drops (30, 20, 15, 5, 2 µl) were placed on the center each spread surface, and top view pictures were taken to show the diameter of droplets by handheld microscope. A side view pictures of the 30 µl of water droplets were also taken at 45- and 90-degree angle. The contact angle of a droplet was measured.

Adherence analysis of pzX

A replicate set of 4 pre-autoclaved vermiculites was soaked with 50 µl of *B. cereus* spores mixed with 50 µl purified pzX (autoclaved) or control. Vermiculites were allowed to air-dry for 24 h. The vermiculites were washed twice with sterile deionized water (DDW) each included a quick dip of a vermiculite 5 times into 1 ml sterile DDW. The DDW wash was discarded and the vermiculites were placed in 1 ml fresh sterile DDW before vortexed (2 min) to release remnant adhered spores. An aliquot of the water containing spores was used for serial dilutions, plated on BHI agar plates, and number CFUs were counted. For pzX titration adherence assays, different amount of pzX (0, 2, 10, 20 µg) were mixed with spores and co-dried with vermiculites prior to washing and plating. Additionally, 100 µl of 5-day Msgg culture including spores and medium was directly co-dried with vermiculites, without any purification of spores or pzX. This adherence test was carried out with *B. cereus* WT and *Δbc0486*.

Analysis of pzX as antiaggregant

B. anthracis Sterne 34F2 and *B. cereus* ATCC 14579 spores isolated from 5 days Msgg medium were heat activated (80 ^{o}C; 20 min) in 0.2 ml of sterile DDW water. The activated spores were incubated for 15 min at 37 ^{o}C in 0.2 ml buffer (10 mM Tris-HCl pH 8, 10 mM NaCl). Subsequently, the spore suspension was supplemented with 30 µl of germinant solution (50 mM inosine dissolved in10 mM Tris-HCl pH 8, 10 mM NaCl), and incubated at 37 °C for 20 min. The germinated spores were washed three times with sterile DDW and incubated in 0.5 ml Msgg salts (Msgg medium lacking glycerol and amino acids) that was supplemented with 20 µg pzX at 30 °C for 2 days. One set of aliquots was used for serial dilutions, and CFUs were counted before and after germination, and 4, 8, 12, 24, 53 h post germination. The second set of aliquots was used to examine cell morphology under phase-contrast microscope. The relative amount of intact pzX remained in the medium was also tested by alditol-acetate derivatization and GC-MS analysis.

Analysis of pzX at different pH

B. anthracis Sterne 34F spores isolated from 5 days Msgg medium was suspended in 0.5 ml of sterile DDW and mixed with or without 100 µg pzX. For acid condition, pH was lowered to 2 by adding 50 mM HCl to a final concentration 10 mM in 0.2 ml of solution. The samples was incubated at 30 °C for 24 hours. To test if pzX precipitates and bioencapsulates spores, the top spores/pzX suspension portion and the bottom clear portion of the sample were aliquoted and tested separately by CFU counts and phase-contrast microscopy. Subsequently samples were vortexed to mix and were plated on BHI agar plates to count the total spore numbers by CFUs.

ACKNOWLEDGEMENTS

We thank Dr. John Glushka, Russ Carlson, Adam Driks and Anne Moir for lively discussion and useful comments on the manuscript.

CONFLICT OF INTEREST

The authors declare that they have no conflicts of interest with the contents of this article.

AUTHOR CONTRIBUTIONS

MBP conceived and coordinated the study. ZL designed, performed and analyzed most of the experiments. Both MBP and ZL wrote the paper. SH performed the initial GC and NMR experiments and provided technical assistance for data analysis and interpretation. All authors reviewed the results and approved the final version of the manuscript.

REFERENCES

1. Cherkasskiy, B. L. (1999) A national register of historic and contemporary anthrax foci. *Journal of applied microbiology* **87**, 192-195
2. Sterne, M. (1939) The use of anthrax vaccines prepared from avirulent (uncapsulated) variants of Bacillus anthracis. *Journal of Veterinary Science and Animal Industry* **13**, 307-312
3. Thapa, N. K., Tenzin, Wangdi, K., Dorji, T., Migma, Dorjee, J., Marston, C. K., and Hoffmaster, A. R. (2014) Investigation and Control of Anthrax Outbreak at the Human-Animal Interface, Bhutan, 2010. *Emerg Infect Dis* **20**, 1524-1526
4. Jernigan, D. B., Raghunathan, P. L., Bell, B. P., Brechner, R., Bresnitz, E. A., Butler, J. C., Cetron, M., Cohen, M., Doyle, T., Fischer, M., Greene, C., Griffith, K. S., Guarner, J., Hadler, J. L., Hayslett, J. A., Meyer, R., Petersen, L. R., Phillips, M., Pinner, R., Popovic, T., Quinn, C. P., Reefhuis, J., Reissman, D., Rosenstein, N., Schuchat, A., Shieh, W. J., Siegal, L., Swerdlow, D. L., Tenover, F. C., Traeger, M., Ward, J. W., Weisfuse, I., Wiersma, S., Yeskey, K., Zaki, S., Ashford, D. A., Perkins, B. A., Ostroff, S., Hughes, J., Fleming, D., Koplan, J. P., Gerberding, J. L., and Investi, N. A. E. (2002) Investigation of bioterrorism-related anthrax, United States, 2001: Epidemiologic findings. *Emerg Infect Dis* **8**, 1019-1028
5. Rasko, D. A., Altherr, M. R., Han, C. S., and Ravel, J. (2005) Genomics of the Bacillus cereus group of organisms. *FEMS microbiology reviews* **29**, 303-329
6. Van der Auwera, G. A., Feldgarden, M., Kolter, R., and Mahillon, J. (2013) Whole-Genome Sequences of 94 Environmental Isolates of Bacillus cereus Sensu Lato. *Genome announcements* **1**
7. Miller, J. M., Hair, J. G., Hebert, M., Hebert, L., Roberts, F. J., and Weyant, R. S. (1997) Fulminating bacteremia and pneumonia due to Bacillus cereus (vol 35, pg 504, 1997). *Journal of clinical microbiology* **35**, 1294-1294
8. Avashia, S. B., Riggins, W. S., Lindley, C., Hoffmaster, A., Drumgoole, R., Nekomoto, T., Jackson, P. J., Hill, K. K., Williams, K., Lehman, L., Libal, M. C., Wilkins, P. P., Alexander, J., Tvaryanas, A., and Betz, T. (2007) Fatal pneumonia among metalworkers due to inhalation exposure to Bacillus cereus containing Bacillus anthracis toxin genes. *Clinical Infectious Diseases* **44**, 414-416
9. Klee, S. R., Ozel, M., Appel, B., Boesch, C., Ellerbrok, H., Jacob, D., Holland, G., Leendertz, F. H., Pauli, G., Grunow, R., and Nattermann, H. (2006) Characterization of Bacillus anthracis-like bacteria isolated from wild great apes from Cote d'Ivoire and Cameroon. *Journal of bacteriology* **188**, 5333-5344
10. Bottone, E. J. (2010) Bacillus cereus, a volatile human pathogen. *Clinical microbiology reviews* **23**, 382-398
11. Hoffmaster, A. R., Ravel, J., Rasko, D. A., Chapman, G. D., Chute, M. D., Marston, C. K., De, B. K., Sacchi, C. T., Fitzgerald, C., Mayer, L. W., Maiden, M. C., Priest, F. G., Barker, M., Jiang, L., Cer, R. Z., Rilstone, J., Peterson, S. N., Weyant, R. S., Galloway, D. R., Read, T. D., Popovic, T., and Fraser, C. M. (2004) Identification of anthrax toxin genes in a Bacillus cereus associated with an illness resembling inhalation anthrax. *Proceedings of the National Academy of Sciences of the United States of America* **101**, 8449-8454

12. Hoffmaster, A. R., Hill, K. K., Gee, J. E., Marston, C. K., De, B. K., Popovic, T., Sue, D., Wilkins, P. P., Avashia, S. B., Drumgoole, R., Helma, C. H., Ticknor, L. O., Okinaka, R. T., and Jackson, P. J. (2006) Characterization of Bacillus cereus isolates associated with fatal pneumonias: strains are closely related to Bacillus anthracis and harbor B. anthracis virulence genes. *Journal of clinical microbiology* **44**, 3352-3360
13. Kolsto, A. B., Tourasse, N. J., and Okstad, O. A. (2009) What Sets Bacillus anthracis Apart from Other Bacillus Species? *Annu Rev Microbiol* **63**, 451-476
14. Girault, G., Blouin, Y., Vergnaud, G., and Derzelle, S. (2014) High-throughput sequencing of Bacillus anthracis in France: investigating genome diversity and population structure using whole-genome SNP discovery. *Bmc Genomics* **15**, 288
15. Derzelle, S., Girault, G., Kokotovic, B., and Angen, O. (2015) Whole Genome-Sequencing and Phylogenetic Analysis of a Historical Collection of Bacillus anthracis Strains from Danish Cattle. *PloS one* **10**, e0134699
16. Inglesby, T. V., Henderson, D. A., Bartlett, J. G., Ascher, M. S., Eitzen, E., Friedlander, A. M., Hauer, J., McDade, J., Osterholm, M. T., O'Toole, T., Parker, G., Perl, T. M., Russell, P. K., Tonat, K., and Biodefense, W. G. C. (1999) Anthrax as a biological weapon - Medical and public health management. *Jama-J Am Med Assoc* **281**, 1735-1745
17. Van Houdt, R., and Michiels, C. (2010) Biofilm formation and the food industry, a focus on the bacterial outer surface. *Journal of applied microbiology* **109**, 1117-1131
18. Nam, H., Seo, H. S., Bang, J., Kim, H., Beuchat, L. R., and Ryu, J. H. (2014) Efficacy of gaseous chlorine dioxide in inactivating Bacillus cereus spores attached to and in a biofilm on stainless steel. *International journal of food microbiology* **188**, 122-127
19. Ryu, J. H., and Beuchat, L. R. (2005) Biofilm formation and sporulation by Bacillus cereus on a stainless steel surface and subsequent resistance of vegetative cells and spores to chlorine, chlorine dioxide, and a peroxyacetic acid-based sanitizer. *Journal of food protection* **68**, 2614-2622
20. Gotz, F. (2002) Staphylococcus and biofilms. *Molecular microbiology* **43**, 1367-1378
21. Lemon, K. P., Earl, A. M., Vlamakis, H. C., Aguilar, C., and Kolter, R. (2008) Biofilm development with an emphasis on Bacillus subtilis. *Current topics in microbiology and immunology* **322**, 1-16
22. Singh, P. K., Schaefer, A. L., Parsek, M. R., Moninger, T. O., Welsh, M. J., and Greenberg, E. P. (2000) Quorum-sensing signals indicate that cystic fibrosis lungs are infected with bacterial biofilms. *Nature* **407**, 762-764
23. Fedtke, I., Gotz, F., and Peschel, A. (2004) Bacterial evasion of innate host defenses - the Staphylococcus aureus lesson. *Int J Med Microbiol* **294**, 189-194
24. Sutherland, I. W. (2001) The biofilm matrix - an immobilized but dynamic microbial environment. *Trends in microbiology* **9**, 222-227
25. Vlamakis, H., Chai, Y., Beauregard, P., Losick, R., and Kolter, R. (2013) Sticking together: building a biofilm the Bacillus subtilis way. *Nature reviews. Microbiology* **11**, 157-168
26. Epstein, A. K., Pokroy, B., Seminara, A., and Aizenberg, J. (2011) Bacterial biofilm shows persistent resistance to liquid wetting and gas penetration. *Proceedings of the National Academy of Sciences of the United States of America* **108**, 995-1000
27. Gu, X. G., Glushka, J., Lee, S. G., and Bar-Peled, M. (2010) Biosynthesis of a New UDP-sugar, UDP-2-acetamido-2-deoxyxylose, in the Human Pathogen Bacillus cereus Subspecies cytotoxis NVH 391-98. *Journal of Biological Chemistry* **285**, 24825-24833
28. Branda, S. S., Gonzalez-Pastor, J. E., Ben-Yehuda, S., Losick, R., and Kolter, R. (2001) Fruiting body formation by Bacillus subtilis. *Proceedings of the National Academy of Sciences of the United States of America* **98**, 11621-11626
29. Severson, K. M., Mallozzi, M., Bozue, J., Welkos, S. L., Cote, C. K., Knight, K. L., and Driks, A. (2009) Roles of the Bacillus anthracis spore protein ExsK in exosporium maturation and germination. *Journal of bacteriology* **191**, 7587-7596

30. Nakata, H. M. (1964) Organic Nutrients Required for Growth and Sporulation of Bacillus Cereus. *Journal of bacteriology* **88**, 1522-1524
31. Hsueh, Y. H., Somers, E. B., Lereclus, D., Ghelardi, E., and Wong, A. C. (2007) Biosurfactant production and surface translocation are regulated by PlcR in Bacillus cereus ATCC 14579 under low-nutrient conditions. *Applied and environmental microbiology* **73**, 7225-7231
32. Fedhila, S., Daou, N., Lereclus, D., and Nielsen-LeRoux, C. (2006) Identification of Bacillus cereus internalin and other candidate virulence genes specifically induced during oral infection in insects. *Molecular microbiology* **62**, 339-355
33. Ellwood, D. C., and Tempest, D. W. (1972) Influence of culture pH on the content and composition of teichoic acids in the walls of Bacillus subtilis. *Journal of general microbiology* **73**, 395-402
34. Hornstra, L. M., de Vries, Y. P., de Vos, W. M., and Abee, T. (2006) Influence of sporulation medium composition on transcription of ger operons and the germination response of spores of Bacillus cereus ATCC 14579. *Applied and environmental microbiology* **72**, 3746-3749
35. Cliff, J. B., Jarman, K. H., Valentine, N. B., Golledge, S. L., Gaspar, D. J., Wunschel, D. S., and Wahl, K. L. (2005) Differentiation of spores of Bacillus subtilis grown in different media by elemental characterization using time-of-flight secondary ion mass spectrometry. *Applied and environmental microbiology* **71**, 6524-6530
36. Purohit, M., Sassi-Gaha, S., and Rest, R. F. (2010) Rapid sporulation of Bacillus anthracis in a high iron, glucose-free medium. *Journal of microbiological methods* **82**, 282-287
37. Clements, M. O., and Moir, A. (1998) Role of the gerI operon of Bacillus cereus 569 in the response of spores to germinants. *Journal of bacteriology* **180**, 6729-6735
38. York, W. S., Darvill, A. G., Mcneil, M., Stevenson, T. T., and Albersheim, P. (1986) Isolation and Characterization of Plant-Cell Walls and Cell-Wall Components. *Methods in enzymology* **118**, 3-40
39. Anumula, K. R., and Taylor, P. B. (1992) A Comprehensive Procedure for Preparation of Partially Methylated Alditol Acetates from Glycoprotein Carbohydrates. *Analytical biochemistry* **203**, 101-108
40. Pereira, P. M., Veiga, H., Jorge, A. M., and Pinho, M. G. (2010) Fluorescent reporters for studies of cellular localization of proteins in Staphylococcus aureus. *Applied and environmental microbiology* **76**, 4346-4353
41. Arnaud, M., Chastanet, A., and Debarbouille, M. (2004) New vector for efficient allelic replacement in naturally nontransformable, low-GC-content, gram-positive bacteria. *Applied and environmental microbiology* **70**, 6887-6891
42. Turgeon, N., Laflamme, C., Ho, J., and Duchaine, C. (2006) Elaboration of an electroporation protocol for Bacillus cereus ATCC 14579. *Journal of microbiological methods* **67**, 543-548
43. Joseph, P., Fantino, J. R., Herbaud, M. L., and Denizot, F. (2001) Rapid orientated cloning in a shuttle vector allowing modulated gene expression in Bacillus subtilis. *FEMS microbiology letters* **205**, 91-97

FOOTNOTES

*This work was supported by the BioEnergy Science Center (grant DE-PS02-06ER64304), which is supported by the Office of Biological and Environmental Research in the Department of Energy (DOE) Office of Science

FIGURE LEGENDS

Figure 1. Comparative analyses of XNAC operon. (**A**) Organization and conserved synteny of genes within the XNAC operon. (**B**) The biochemical pathway for the conversion of UDP-GlcNAc to UDP-XylNAc by UGlcNAcDH and UXylNAcS (27) within the XNAC operon are illustrated. A phylogenetic tree of UXylNAcS (**C**) depicts that XNAC operon is only present in members of the *Bacillus cereus* sensu lato group. Strains marked with * are the lines that were used to analyze pzX in this study.

Figure 2. pzX is a secreted polysaccharide and induced to form when strains belonging to *Bacillus cereus* group are growing in Msgg nutrient medium. **A**. Genes of the XNAC operon are co-transcribed and the expression is induced during growth of *B. thuringiensis* in Msgg liquid medium but not in LB or BHI medium. RT-PCR analysis for the expression of gene encoding: lane 1, putative glycosyltransferase; lane 2, UGlcNAcDH; lane 3, UXylNAcS; lane 4, putative glycosyltransferase; lane P, sigA positive control; lane N, negative control (RT reaction without added primers). GC-MS analyses of alditol-acetate derivatives of (**B**) crude pzX of *B. thuringiensis* israelensis grown in Msgg and BHI medium (lower panel); of (**C**) *B. cereus* and *B. subtilis* (lower panel) grown in Msgg medium; of (**D**) purified $pzX^{bc14579}$. Panel (**E**) shows the GC-MS spectra of *B. cereus* wild-type (WT), glycosyltransferase deletion (*Δbc0486)* and complemented strains (complemented *Δbc0486)* Note a single peak X (denote XylNAc) of borodeuterated-XylNAc-alditol-acetate-derivative. Peak '*' denotes an unknown sugar peak. Peak 'a' denotes an unknown but non-sugar peak. The EI-MS with *m/z* ion fragments of peak XylNAc (X) is shown in the left boxed area; and the right boxed insert shows the predicted primary and secondary MS fragments of C1-deuterated alditol-acetate of derived XylNAc; (**F**) non-deuterated XylNAc-alditol-acetate-derivative obtained from *B. cereus* cells fed with [C2-^{13}C]glycerol and yielded ^{13}C-2,5 labeled $pzX^{bc14579}$. Note the addition of 2 mass units to alditol-acetate derivative due to incorporation of two ^{13}C per XylNAc (e.g. 288 ->290).

Figure 3. A proposed chemical structure of pzX. **A.** pzX consists of Xyl*p*NAc(4OAc) (denote A) α-1,3 linked to Glc*p*NAcA(4OAc) (denote C) that is α-1,3 linked to Xyl*p*NAc (denote B). One-dimensional proton NMR spectrum (**B**) of purified $pzX^{bc14579}$; and one-dimensional carbon-13 NMR spectrum (**C**), is shown. Protons belonging to each anomeric region are labeled "H-1" and the signals and chemical shifts for the three sugar residues carbon anomeric region (C-1) are shown in the boxed insert.

Figure 4. 2D-NMR revealed pzX consists of three sugars with XylNAc and GlcNAcA configurations. The partial HMQC NMR spectrum of ^{13}C-2,5 labeled pzX showing **A**) protons bond to carbon 5, in residues A, B, C [CH-5]; (**B**) protons bond to carbon two in residues A, B, C [CH-2 region]. The partial HMQC-TOCSY spectrum (**C**) of ^{13}C-2,5 labeled pzX depicts a unique H4 chemical shifts of the proton in residue A and C, implying 4-O substitution. An INADEQUEATE ^{13}C-^{13}C NMR experiment (**D**) of 13C fully labeled pzX shows residue C has a connectivity of C5 to another carbon C6, with carbon chemical shift of a carbonyl. The NMR multiplicity-edited HSQC experiment (**E**) of pzX depicts carbon five (C5) of residue C only have one proton (phase red) whereas C5 of residue A and B have two protons (phase blue) implying residue A and B have *xylo*-configuration with two hydrogens linked to C5 and residue C is a 6-ring sugar with carboxylate at C6. The HMBC experiment of de-O-acetylated pzX (**F**) illustrates connectivity of C6 to H4 and H5 of residue C. Dionex HPLC- PAD spectrum (**G**) of TFA-hydrolyzed pzX (lower panel) gave two peaks, one eluted as neutral sugar (~9 min) and the other (~26 min) eluted as charged sugar. Label * indicates buffer contamination.

Figure 5. Residue A and C in pzX are 4-O-acetylated. Partial HMBC NMR spectrum (**A**) of ^{13}C-2,5 labeled pzX illustrates connectivity of carbon from OAc carbonyl group to protons of OAc methyl group and to the H4 in residues A and C. The partial multiplicity-edited HSQC experiment (**B**) of de-O-acetylated pzX illustrates the CH-4 proton belonging to A and C residues are shifted from their position (dotted circle denotes the chemical shifts before de-O-acetylation) to a regular non-substituted sugar ring

region (pointed with arrow). Comparative analysis of partial spectrum of one-dimensional proton NMR is shown (**C**) before and after de-O-acetylation. Note the methyl region of acetate moieties (dotted rectangular box) is significantly reduced upon removal of OAc group.

Figure 6. PMAA and NMR analyses of pzX revealed sugars are linked alpha 1-3 and sugar sequence is A-C-B. GC-MS **(A)** of partially permethylated alditol acetate (PMAA) has a single peak at 27.3 min with *m/z* ion fragments shown in panel (**B**). The boxed insert in B indicates the primary and secondary MS ion fragments depicting that XylNAc is linked at position 3. The partial HSQC-NOESY NMR spectrum (**C**) of de-O-acetylated pzX shows NOE cross peaks of H1- H2 in all three residues, indicative of alpha linked residues; and (**D**) shows 1-3 linkage and connectivity of anomeric carbon (C1) to proton along the glycosidic linkages with cross peaks of C1 of residue A to H3 of residue C, C1 of residue C to H3 of residue B, C1 of residue B to H3 of residue A. A carbon-proton inter-residue cross peaks (**E**) were detected in the HMBC experiments of ^{13}C fully labeled pzX further confirming the linkage and sugar order of pzX is –A(*α-1,3*)B*(α-1,3*)C*(α-1,3)*A–.

Figure 7. GC and NMR spectral overlay of pzX from *B. cereus* ATCC 14579, *B. cereus* ATCC 10876 and *B. anthracis* Sterne 34F2. **A**. GC-MS analyses of alditol-acetate derivatives of crude pzX of three *Bacillus* strains grown in Msgg. 1D proton NMR (**B**) and TOCSY experiment (**C**) spectral overlay of purified pzX from three *Bacillus* strains.

Figure 8. Analyses of pzX produced during sporulation. Cells of *B. cereus* ATCC 14579 grown in Msgg from 8 hours to 6 days were analyzed by phase-contrast microscopy (**A**) and the relative amount of spores and amount of pzX (**B**- Left panel), as well as culture OD_{600} and pH (**B**- right panel) are indicated. Various amounts of pzX and spores were produced in other media (**C**). Variable amount of pzX is produced when Msgg medium is supplemented by increasing amounts of rich medium components or glucose (**D**). Note high level of nutrients media did not support mature spore formations nor did pzX formation. Note: CDS is CDS-Glc medium; M-Temp is modified Tempest medium.

Figure 9. pzX has surfactant properties. *B. cereus* ATCC 14579 planktonic cells and spores spotted on Msgg agar plates previously layered with pzX (lower) or water (upper panel, control) developed a wider colony morphology within 48 hours compared to control (**A**). Drop of water collapsed on a flat polystyrene surface previously spread with native pzX, de-O-acetylated, or autoclaved pzX compared to the surface with water or 0.5% SDS as control. The contact angle of each sample is diagramed below (**B**). Various amount of water (30, 20, 15, 10, 5, 2 µl) collapsed on polystyrene surface spread with native pzX, de-O-acetylated, or autoclaved pzX compared to the surface with water or 0.5% SDS as control (**C**).

Figure 10. Other properties of pzX. Panel A shows the role of pzX in spore adherence. Purified spores of *B. cereus* ATCC 14579 wild type were mixed with or without purified pzX; dried on vermiculites; washed and the remnant attached spores were counted by CFUs (**A, left**). Adherence is concentration dependent (**A, middle**). In addition, culture medium of *B. cereus* WT and *Δbc0486* mutant grown for 5 days in Msgg were directly added to vermiculites without any purification, and the adherence was compared (**A, right**). Panels B, C show pzX as an antiaggregant. Germinated *B. anthracis* Sterne spores were incubated with or without 20 µg pzX for 2 days, and phase-contrast microscopy shows pzX disperses spores (**B**) and in addition enhances number of CFUs (**C**). Panels D, E, F, G provide evidence for pzX role in a film-like matrix formation at environment with low pH. *B. anthracis* spores mixed with or without pzX show the formation of cotton fluff-like floating structure (**D**). Note the UP and DOWN bracket indicates region above or below the 'fluff'. CFUs from the UP and DOWN regions show that spores are associated with the fluff pzX structure (**E**). Phase-contrast microscopy shows a film-like structure of pzX with spores embedded (**F**). Total CFU of spores after vortexing (panel D) and plating on BHI agar shows that spores within this structure are not aggregated (**G**).

TABLES

Table 1. Comparison of pzX production among Bacillus strains

***Bacillus* strains**	**XNAC operon in genome**	**[a]XylNAc production in Msgg medium**	**[b]XylNAc production in BHI medium**
B. thuringiensis israelensis ATCC 35646	Yes	6.8	ND
B. thuringiensis berliner ATCC 10792	Yes	5.1	ND
B. thuringiensis kurstaki HD73	Yes	7.5	ND
B. cereus ATCC 14579	Yes	228	ND
B. cereus ATCC 10876	Yes	493	ND
B. anthracis 34F2	Yes	154	ND
B. subtilis PY79	No	ND	ND
B. megaterium QMB1551	No	ND	ND

a. The relative amount of crude pzX in the medium was estimated after GC-MS analyses by peak integration and ratio of XylNAc and the internal std. inositol.
b. ND not detected under our standard procedure.

Table 2. Chemical shifts of pzX polymer components. Data was acquired in NMR 600Hz at 65 ^{o}C in D2O. DSS was used as reference.

Chemical shifts in ppm	**A 4-OAc-XylNAc**		**B XylNAc**		**C 4-OAc-GlcNAcA**	
Ring Position	**^{1}H**	**^{13}C**	**^{1}H**	**^{13}C**	**^{1}H**	**^{13}C**
1	5.05	99.41	5.06	100.14	5.24	100.88
2	4.07	53.92	3.99	54.43	4.15	54.79
3	3.85	76.10	3.62	81.45	4.00	75.57
4	4.95	75.42	3.84	72.74	5.10	76.22
5a	3.81	60.70	3.68	64.33	3.94	73.09
5b	3.43		3.40		--	--
6	--	--	--	--	--	176.41
Substitution						
C=O O-Ac	--	175.22	--	--	--	174.85
CH3 O-Ac	2.04	23.00	--	--	2.03	23.20
C=O N-Ac	--	176.61	--	176.61		176.61
CH3 N-Ac	1.97	25.00	1.98	25.14	1.99	25.23

Table 3. Chemical shifts of de-O-Ac pzX. Data was acquired in NMR 600Hz at 65 ^{o}C in D2O. DSS was used as reference.

Chemical shifts in ppm	**A XylNAc**		**B XylNAc**		**C GlcNAcA**	
Ring Position	**^{1}H**	**^{13}C**	**^{1}H**	**^{13}C**	**^{1}H**	**^{13}C**
1	5.12	101.47	5.06	101.72	5.21	100.99
2	3.97	55.06	3.95	54.98	4.01	54.76
3	3.61	82.12	3.72	81.01	3.71	81.38
4	3.81	72.92	3.81	73.06	3.87	74.22
5a	3.65	64.50	3.64	64.50	3.73	75.33
5b	3.45		3.45			
6	--		--		--	178.73
Substitution						
C=O N-Ac	--	176.66	--	176.66		176.75
CH3 N-Ac	2.01	24.857	2.01	24.857	1.97	25.23

FIGURE 1

A

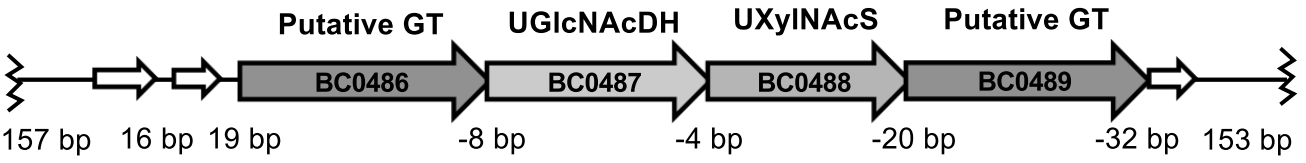
Bacillus cereus ATCC 14579
Putative GT
UGlcNAcDH
UXylNAcS
Putative GT
BC0486
BC0487
BC0488
BC0489
157 bp
16 bp
19 bp
-8 bp
-4 bp
-20 bp
-32 bp
153 bp

B

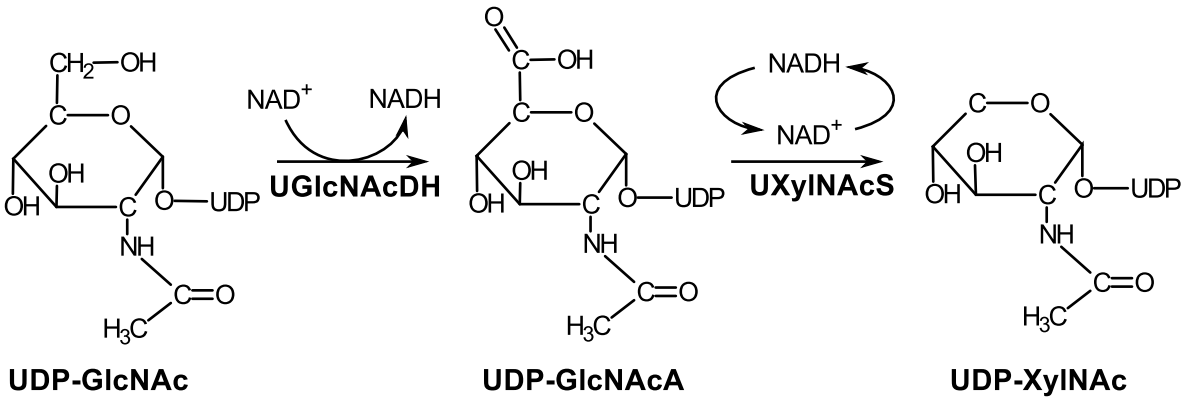
NAD+
NADH
UGlcNAcDH
NADH
NAD+
UXylNAcS
UDP-GlcNAc
UDP-GlcNAcA
UDP-XylNAc

C

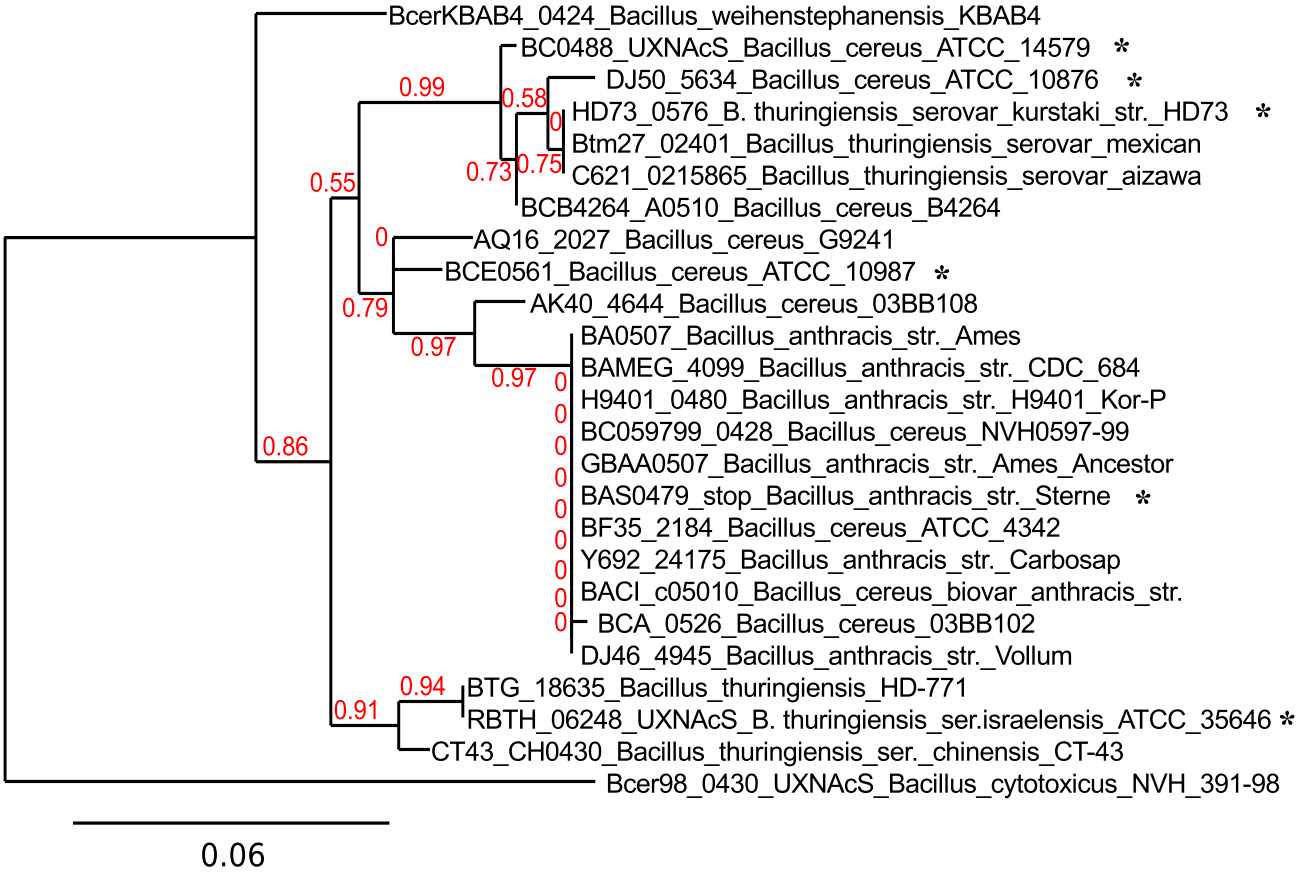
BcerKBAB4_0424_Bacillus_weihenstephanensis_KBAB4
BC0488_UXNAcS_Bacillus_cereus_ATCC_14579 *
DJ50_5634_Bacillus_cereus_ATCC_10876 *
HD73_0576_B. thuringiensis_serovar_kurstaki_str._HD73 *
Btm27_02401_Bacillus_thuringiensis_serovar_mexican
C621_0215865_Bacillus_thuringiensis_serovar_aizawa
BCB4264_A0510_Bacillus_cereus_B4264
AQ16_2027_Bacillus_cereus_G9241
BCE0561_Bacillus_cereus_ATCC_10987 *
AK40_4644_Bacillus_cereus_03BB108
BA0507_Bacillus_anthracis_str._Ames
BAMEG_4099_Bacillus_anthracis_str._CDC_684
H9401_0480_Bacillus_anthracis_str._H9401_Kor-P
BC059799_0428_Bacillus_cereus_NVH0597-99
GBAA0507_Bacillus_anthracis_str._Ames_Ancestor
BAS0479_stop_Bacillus_anthracis_str._Sterne *
BF35_2184_Bacillus_cereus_ATCC_4342
Y692_24175_Bacillus_anthracis_str._Carbosap
BACI_c05010_Bacillus_cereus_biovar_anthracis_str.
BCA_0526_Bacillus_cereus_03BB102
DJ46_4945_Bacillus_anthracis_str._Vollum
BTG_18635_Bacillus_thuringiensis_HD-771
RBTH_06248_UXNAcS_B. thuringiensis_ser.israelensis_ATCC_35646 *
CT43_CH0430_Bacillus_thuringiensis_ser._chinensis_CT-43
Bcer98_0430_UXNAcS_Bacillus_cytotoxicus_NVH_391-98
0.99
0.58
0
0.73
0.75
0.55
0
0.79
0.97
0.97
0
0
0
0
0
0
0
0
0
0.86
0.94
0.91
0.06

FIGURE 2

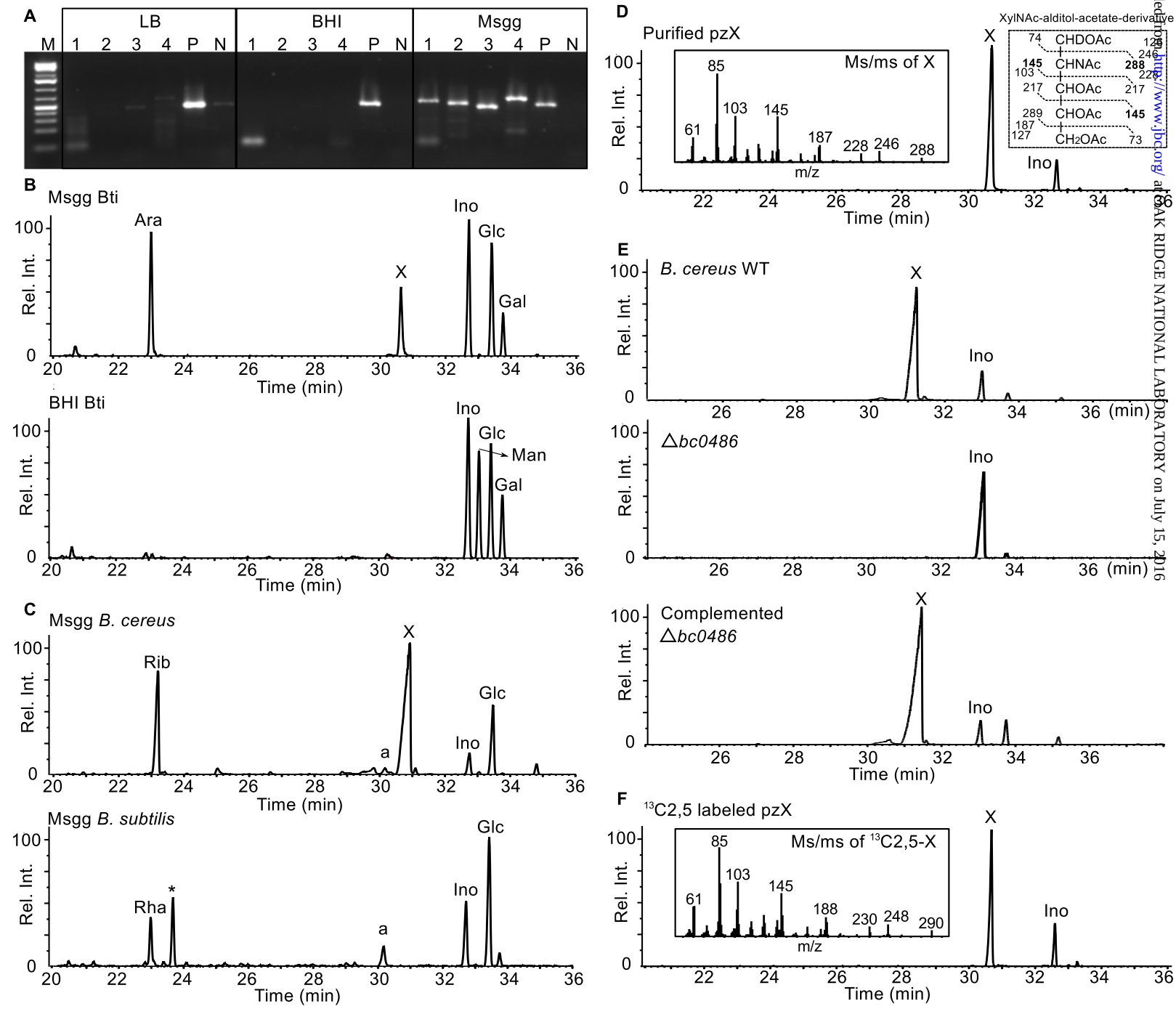

FIGURE 3

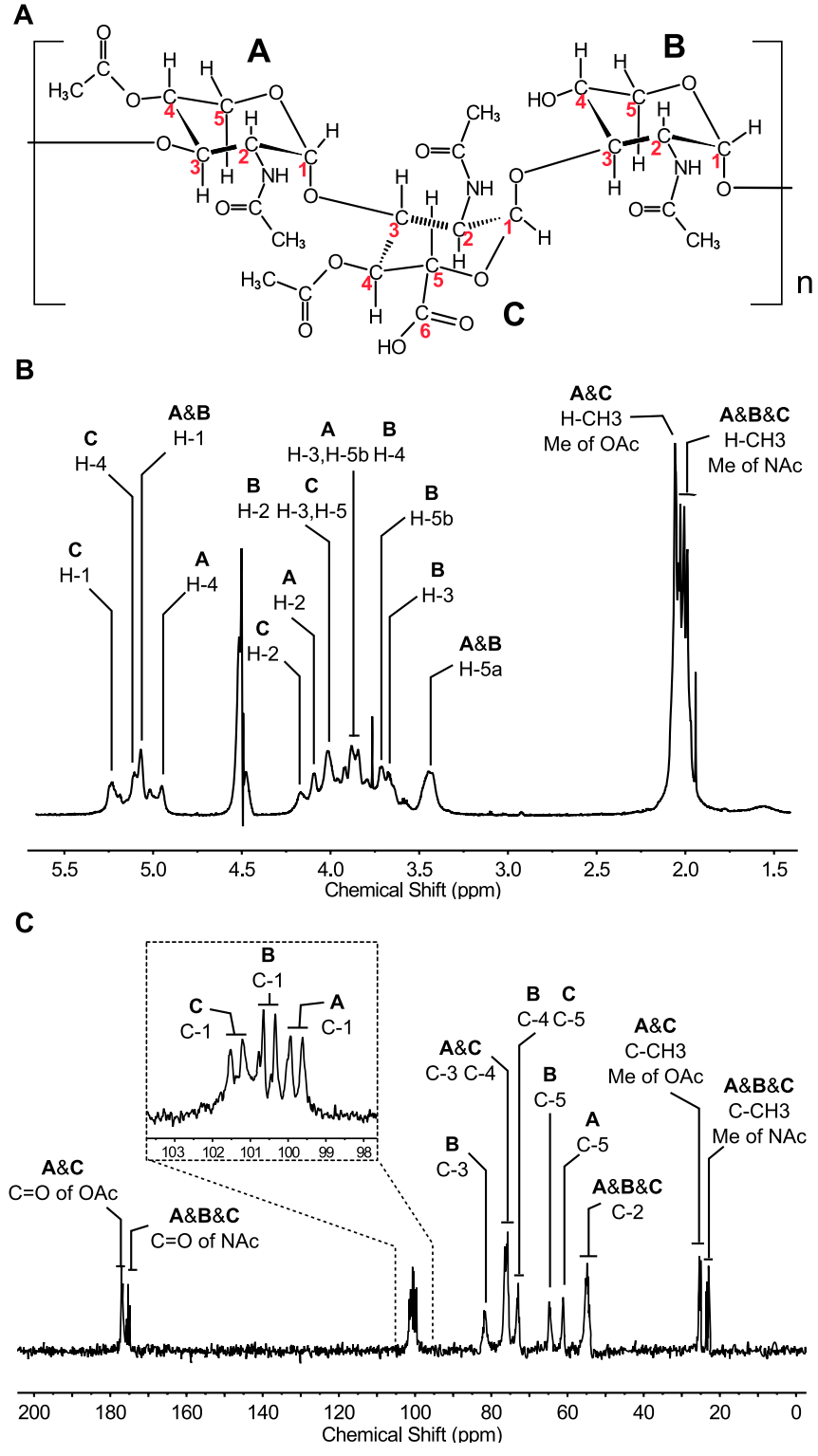
A
B
C
n
B
A&B H-1
C H-4
C H-1
A H-4
B H-2
C H-3,H-5
A H-3,H-5
B H-4
B H-5b
B H-3
A H-2
C H-2
A&B H-5a
A&C H-CH3 Me of OAc
A&B&C H-CH3 Me of NAc
5.5 5.0 4.5 4.0 3.5 3.0 2.5 2.0 1.5
Chemical Shift (ppm)
C
B C-1
C C-1
A C-1
103 102 101 100 99 98
A&C C=O of OAc
A&B&C C=O of NAc
A&C C-3 C-4
B C-4 C-5
B C-5
B C-3
A C-5
A&B&C C-2
A&C C-CH3 Me of OAc
A&B&C C-CH3 Me of NAc
200 180 160 140 120 100 80 60 40 20 0
Chemical Shift (ppm)

FIGURE 4

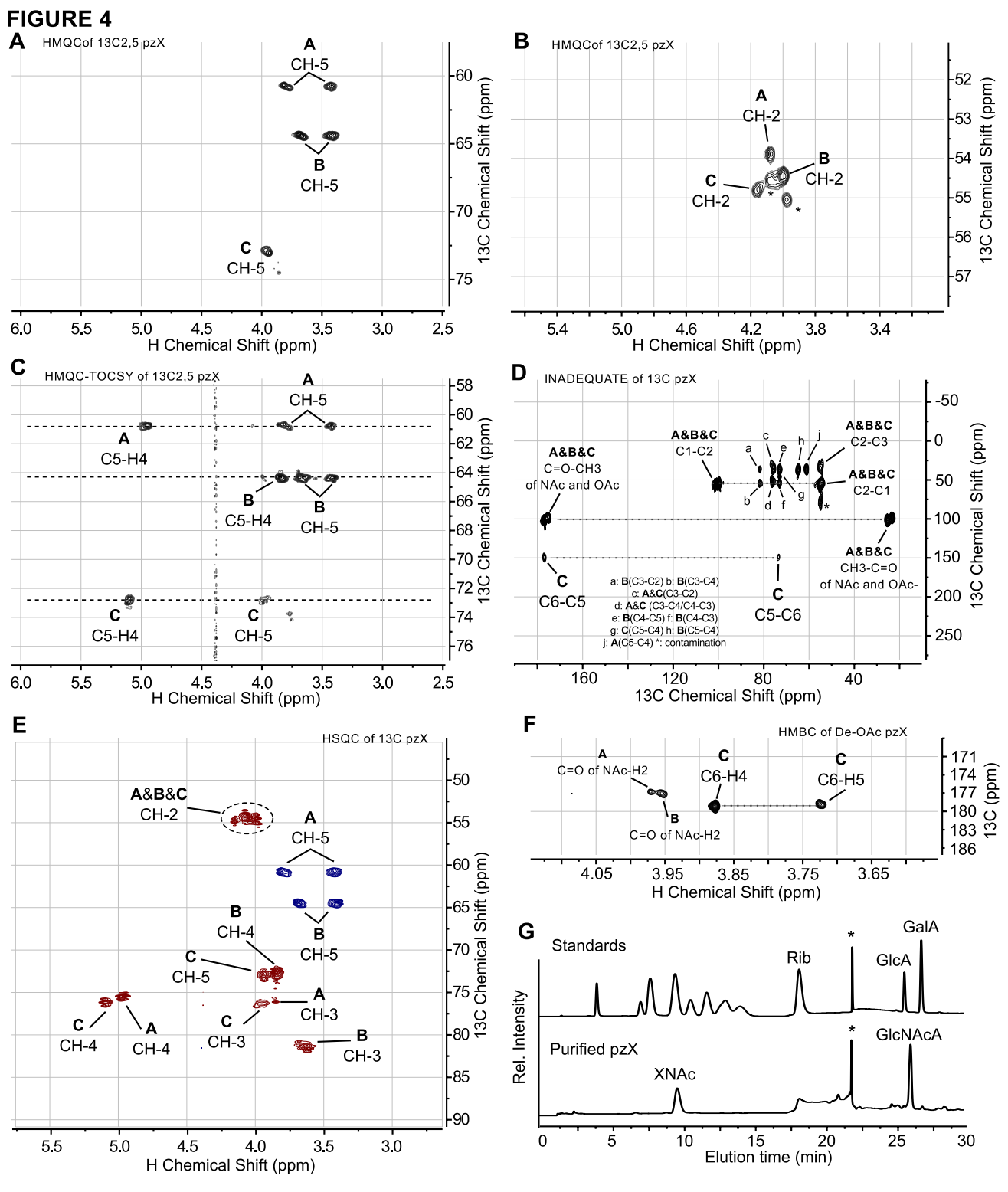
A
HMQCof 13C2,5 pzX
A CH-5
B CH-5
C CH-5
13C Chemical Shift (ppm)
H Chemical Shift (ppm)
B
HMQCof 13C2,5 pzX
A CH-2
B CH-2
C CH-2
C
HMQC-TOCSY of 13C2,5 pzX
A C5-H4
B C5-H4
C C5-H4
D
INADEQUATE of 13C pzX
A&B&C C=O-CH3 of NAc and OAc
A&B&C C1-C2
A&B&C C2-C3
A&B&C C2-C1
A&B&C CH3-C=O of NAc and OAc-
C C6-C5
C C5-C6
a: B(C3-C2) b: B(C3-C4)
c: A&C(C3-C2)
d: A&C (C3-C4/C4-C3)
e: B(C4-C5) f: B(C4-C3)
g: C(C5-C4) h: B(C5-C4)
j: A(C5-C4) *: contamination
E
HSQC of 13C pzX
A&B&C CH-2
F
HMBC of De-OAc pzX
A C=O of NAc-H2
B C=O of NAc-H2
C C6-H4
C C6-H5
G
Standards
Rib
GlcA
GalA
Purified pzX
XNAc
GlcNAcA
Rel. Intensity
Elution time (min)

FIGURE 5

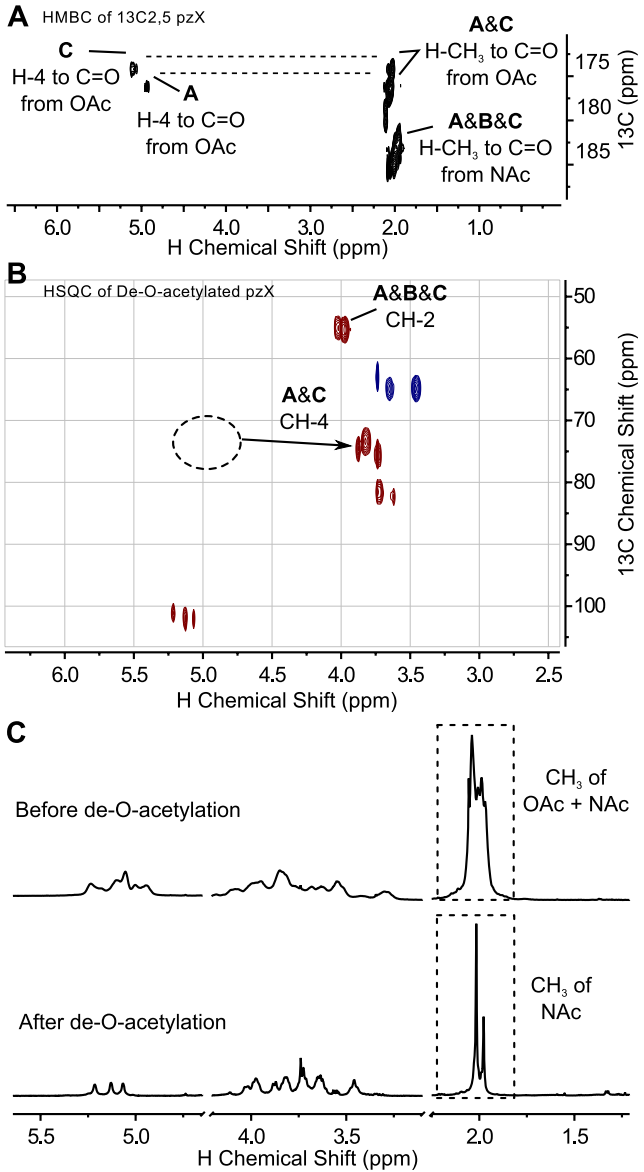
A
HMBC of 13C2,5 pzX
C
H-4 to C=O
from OAc
A
H-4 to C=O
from OAc
A&C
H-CH3 to C=O
from OAc
A&B&C
H-CH3 to C=O
from NAc
175
180
185
13C (ppm)
6.0
5.0
4.0
3.0
2.0
1.0
H Chemical Shift (ppm)
B
HSQC of De-O-acetylated pzX
A&B&C
CH-2
A&C
CH-4
50
60
70
80
90
100
13C Chemical Shift (ppm)
6.0
5.5
5.0
4.5
4.0
3.5
3.0
2.5
H Chemical Shift (ppm)
C
Before de-O-acetylation
CH3 of
OAc + NAc
After de-O-acetylation
CH3 of
NAc
5.5
5.0
4.0
3.5
2.0
1.5
H Chemical Shift (ppm)

FIGURE 6

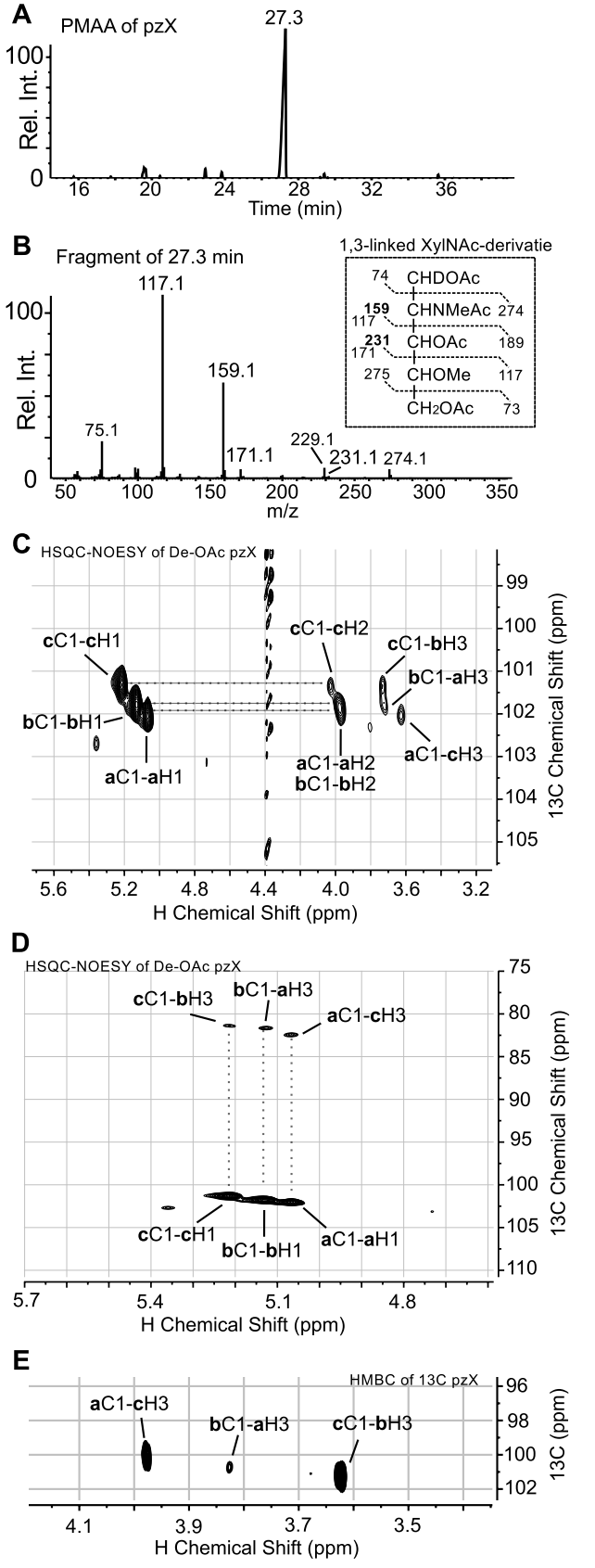
A
PMAA of pzX
27.3
Rel. Int.
Time (min)
B
Fragment of 27.3 min
1,3-linked XylNAc-derivatie
74 CHDOAc
159 CHNMeAc 274
117
231 CHOAc 189
171
275 CHOMe 117
CH2OAc 73
117.1
159.1
75.1
171.1
229.1
231.1
274.1
Rel. Int.
m/z
C
HSQC-NOESY of De-OAc pzX
cC1-cH1
cC1-cH2
cC1-bH3
bC1-aH3
bC1-bH1
aC1-cH3
aC1-aH2
bC1-bH2
aC1-aH1
H Chemical Shift (ppm)
13C Chemical Shift (ppm)
D
HSQC-NOESY of De-OAc pzX
cC1-bH3
bC1-aH3
aC1-cH3
cC1-cH1
bC1-bH1
aC1-aH1
H Chemical Shift (ppm)
13C Chemical Shift (ppm)
E
HMBC of 13C pzX
aC1-cH3
bC1-aH3
cC1-bH3
H Chemical Shift (ppm)
13C (ppm)

FIGURE 7

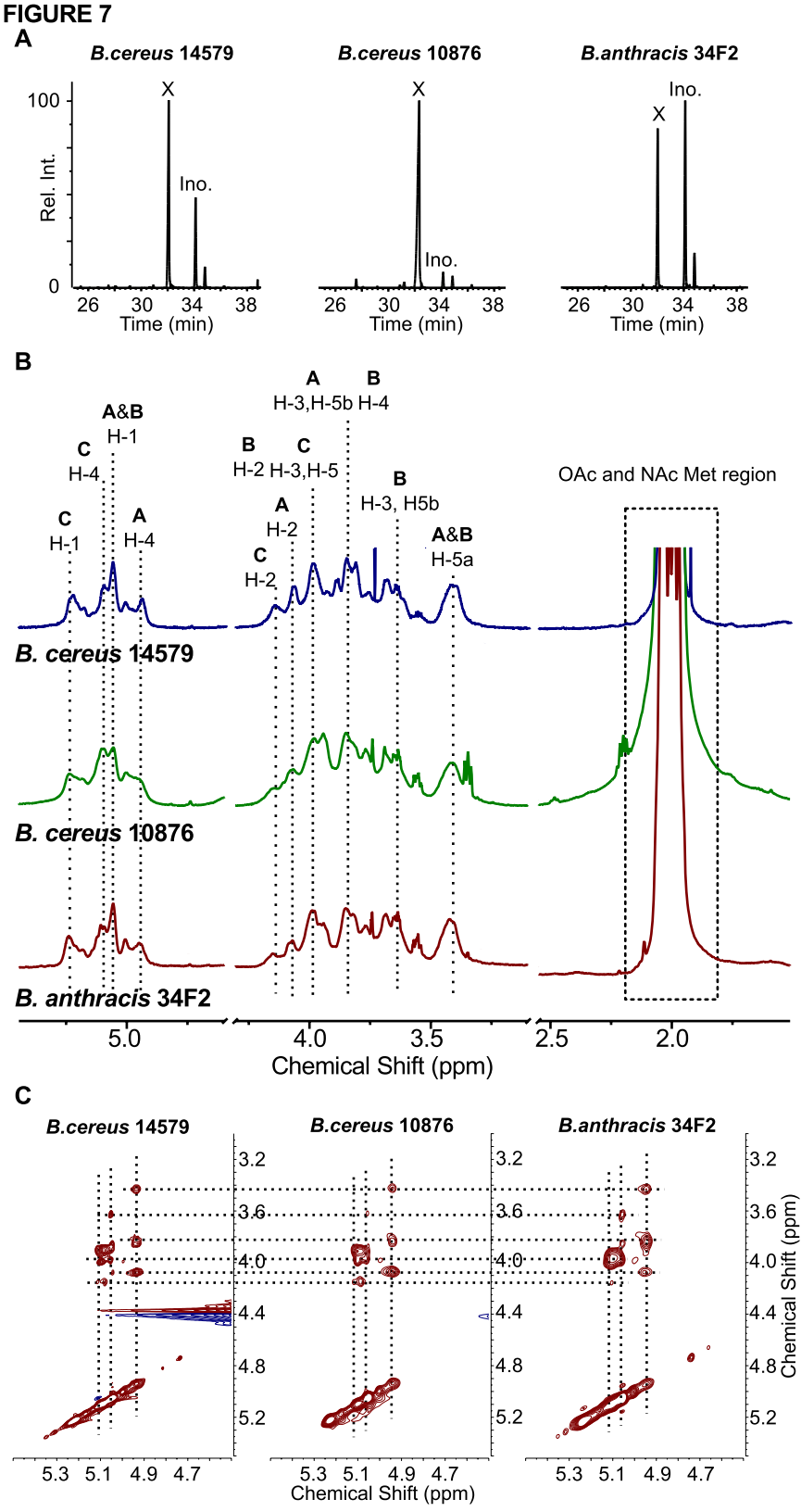
A
B.cereus 14579
B.cereus 10876
B.anthracis 34F2
100
0
Rel. Int.
X
Ino.
26
30
34
38
Time (min)
B
A&B
H-1
C
H-4
C
H-1
A
H-4
A
B
H-3,H-5b H-4
B
H-2 C
H-3,H-5
A
H-2
C
H-2
B
H-3, H5b
A&B
H-5a
OAc and NAc Met region
B. cereus 14579
B. cereus 10876
B. anthracis 34F2
5.0
4.0
3.5
2.5
2.0
Chemical Shift (ppm)
C
B.cereus 14579
B.cereus 10876
B.anthracis 34F2
3.2
3.6
4.0
4.4
4.8
5.2
5.3
5.1
4.9
4.7
Chemical Shift (ppm)

FIGURE 8

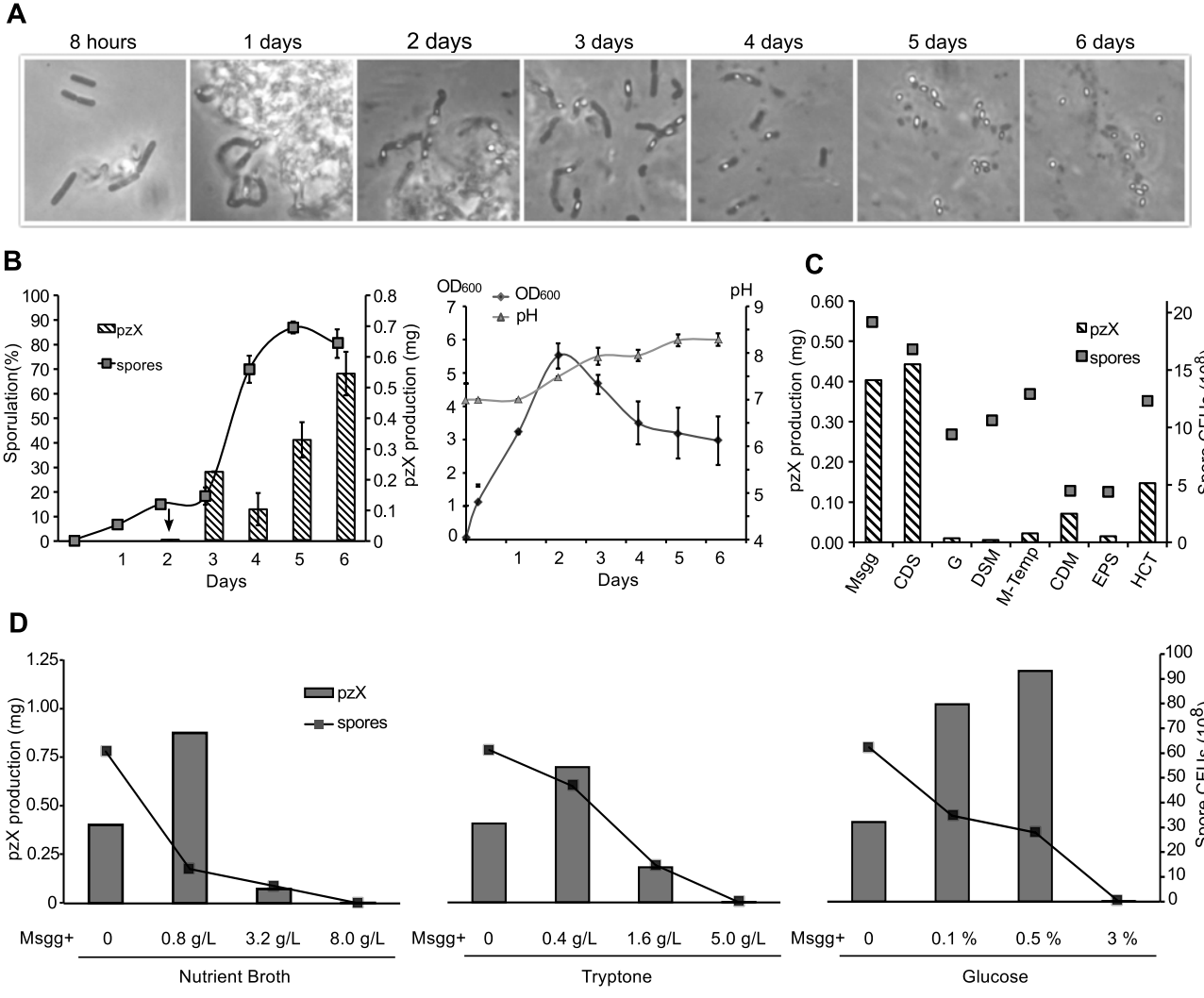
A
8 hours
1 days
2 days
3 days
4 days
5 days
6 days
B
Sporulation(%)
pzX
spores
pzX production (mg)
Days
OD600
pH
C
pzX production (mg)
Spore CFUs (10^8)
Msgg
CDS
G
DSM
M-Temp
CDM
EPS
HCT
D
pzX production (mg)
Spore CFUs (10^8)
Msgg+ 0 0.8 g/L 3.2 g/L 8.0 g/L
Nutrient Broth
Msgg+ 0 0.4 g/L 1.6 g/L 5.0 g/L
Tryptone
Msgg+ 0 0.1 % 0.5 % 3 %
Glucose

FIGURE 9

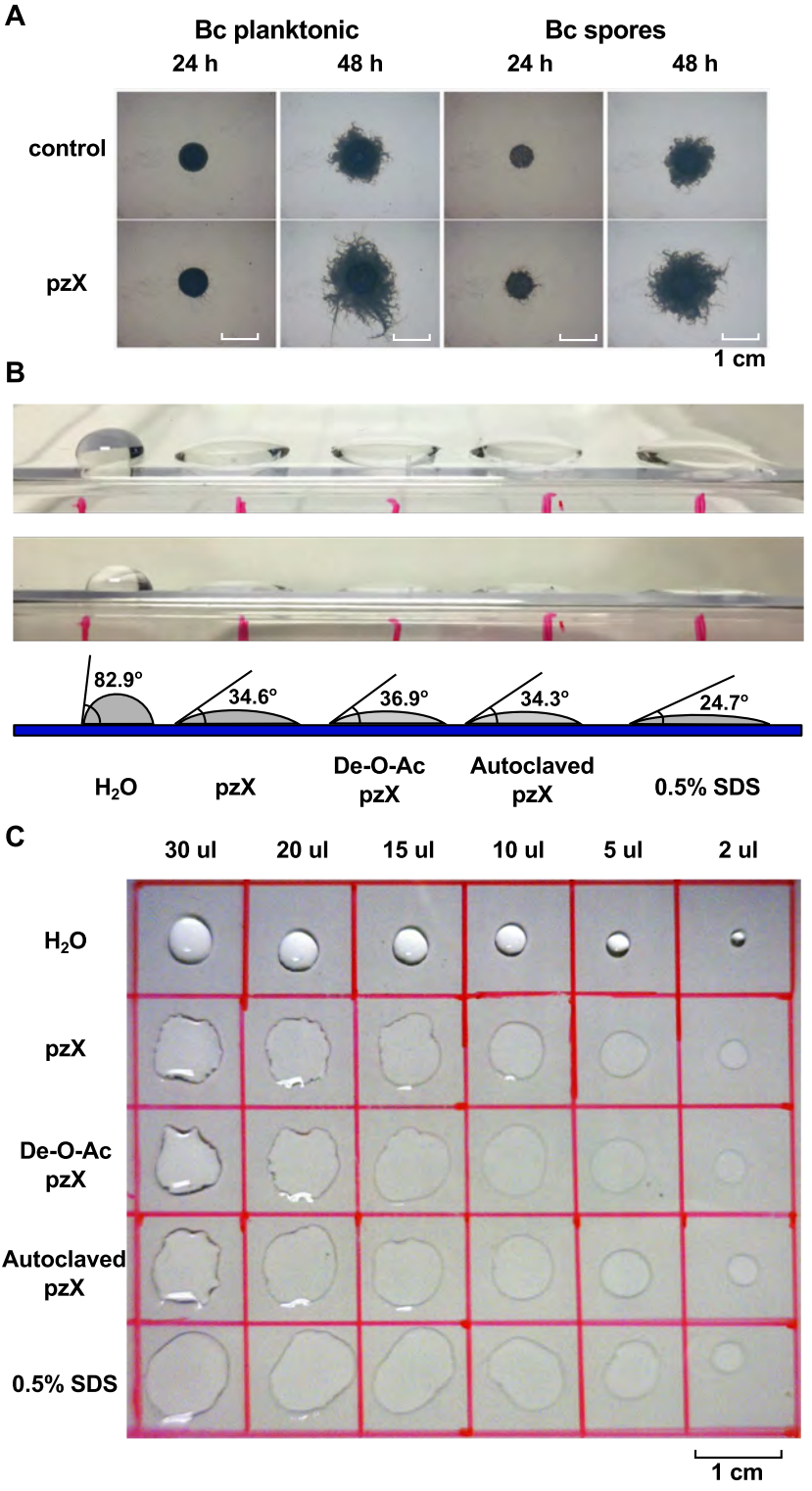
A
Bc planktonic
Bc spores
24 h
48 h
24 h
48 h
control
pzX
1 cm
B
82.9°
34.6°
36.9°
34.3°
24.7°
H2O
pzX
De-O-Ac pzX
Autoclaved pzX
0.5% SDS
C
30 ul
20 ul
15 ul
10 ul
5 ul
2 ul
H2O
pzX
De-O-Ac pzX
Autoclaved pzX
0.5% SDS
1 cm

FIGURE 10

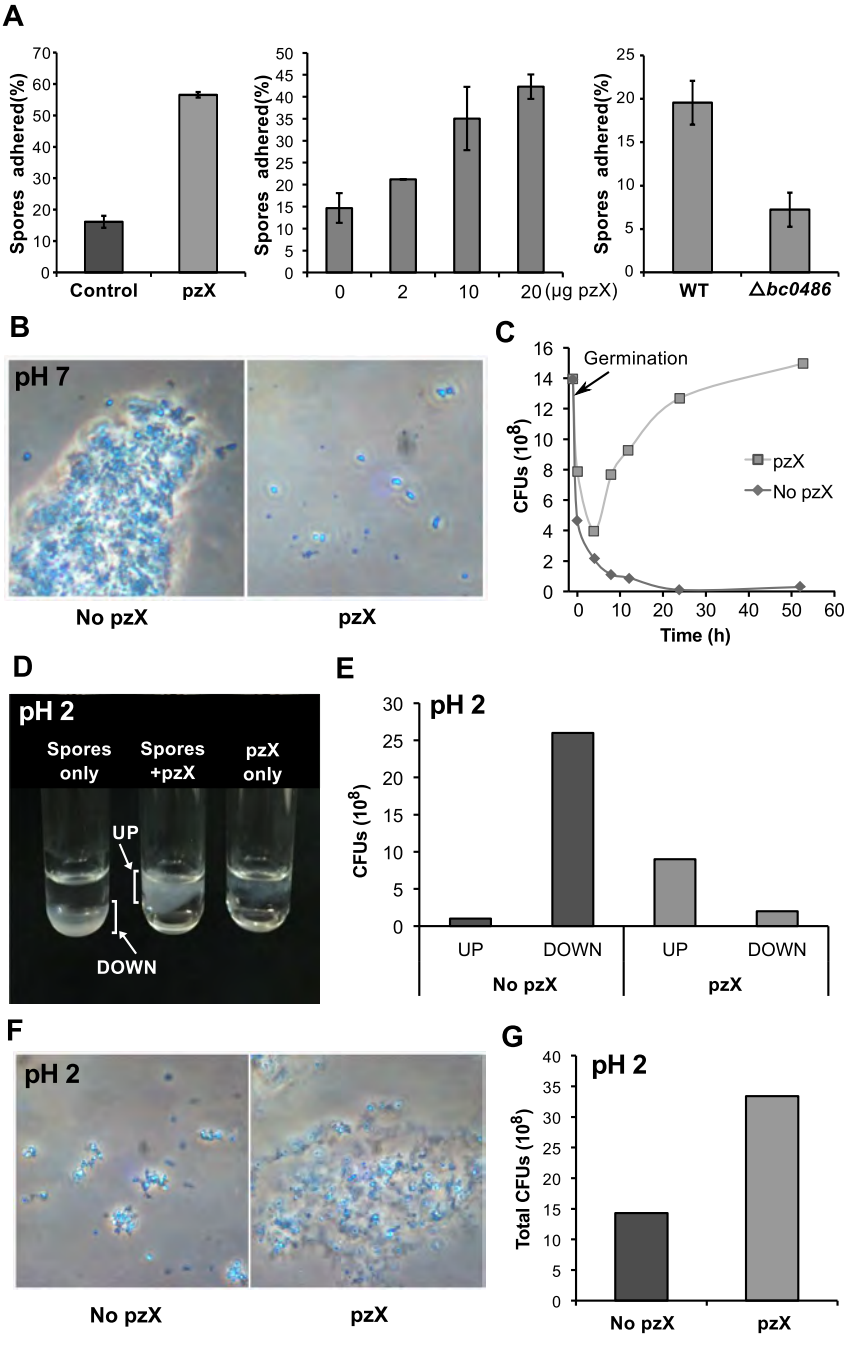
A
Spores adhered(%)
Control
pzX
0
2
10
20 (µg pzX)
WT
Δbc0486
B
pH 7
No pzX
pzX
C
Germination
CFUs (10^8)
pzX
No pzX
Time (h)
D
pH 2
Spores only
Spores +pzX
pzX only
UP
DOWN
E
pH 2
CFUs (10^8)
UP
DOWN
No pzX
pzX
F
pH 2
No pzX
pzX
G
pH 2
Total CFUs (10^8)
No pzX
pzX

Discovery of a unique extracellular polysaccharide in members of the pathogenic bacillus that can co-form with spores

Zi Li, Soyoun Hwang and Maor Bar-Peled

J. Biol. Chem. published online July 11, 2016
